UNCLASSIFIED

AD 273 051

Reproduced
by the

ARMED SERVICES TECHNICAL INFORMATION AGENCY
ARLINGTON HALL STATION
ARLINGTON 12, VIRGINIA

UNCLASSIFIED

NOTICE: When government or other drawings, specifications or other data are used for any purpose other than in connection with a definitely related government procurement operation, the U. S. Government thereby incurs no responsibility, nor any obligation whatsoever; and the fact that the Government may have formulated, furnished, or in any way supplied the said drawings, specifications, or other data is not to be regarded by implication or otherwise as in any manner licensing the holder or any other person or corporation, or conveying any rights or permission to manufacture, use or sell any patented invention that may in any way be related thereto.

CATALOGED BY ASTIA
AS AD NO. 273051
273 051

ASTIA
RECEIVED
MAR 19 1962
TISIA B

PRINCETON UNIVERSITY

DEPARTMENT OF AERONAUTICAL ENGINEERING

U. S. Army Transportation Research Command
Fort Eustis, Virginia

Project Number: 9-38-10-000, TK902
Contract Number: DA44-177-TC-524

MODEL STUDIES OF THE FORWARD FLIGHT CHARACTERISTICS OF THE P-GEM

by

M. P. Knowlton and A. F. Wojciechowicz, Jr.

Department of Aeronautical Engineering
Princeton University

Report No. 581 December, 1961

Agencies within the Department of Defense and their contractors may obtain copies of this report on a loan basis from:

Armed Services Technical
Information Agency
Arlington Hall Station
Arlington 12, Virginia

Others may obtain copies from:

Office of Technical Services
Acquisition Section
Department of Commerce
Washington 25, D. C.

The views contained in this report are those of the contractor and do not necessarily reflect those of the Department of the Army. The information contained herein will not be used for advertising purposes.

Approved by:

C. D. Perkins

C. D. Perkins, Chairman
Department of Aeronautical
Engineering, Princeton University

SUMMARY

A wind tunnel investigation using a conventional ground board setup has been conducted to determine the forward flight characteristics of a $\frac{1}{12}$ scale model of the P-GEM both within and outside the proximity of the ground. Separate studies were also made of the model with non-blowing wings attached at several locations around its perimeter and also with the addition of a tail. The results show, for all configurations, increases in lift curve slope and reductions in induced drag as the ground was approached. It was also found that the longitudinal static stability could be significantly increased with the addition of properly located wings or a tail.

Forward flight simulation studies were made in the Princeton Forward Flight Facility using a $\frac{1}{5}$ scale model of the P-GEM. Fixed pitch runs determined that the percentage loss in flying height with forward motion was primarily a function of velocity. At the higher velocities the model began to transist into a take-off. During this transition the model was found to be marginally stable or slightly unstable in height. Pitch free runs determined that pitch trim angle increases with flying height, and also pitch instability in hover and flying occurred at about the same height.

Smoke studies were made in the Princeton 4 x 3 foot smoke tunnel to investigate the vortex formation and streamline flow at various dynamic to base pressure ratios. The observations show that at low $\frac{q}{P_b}$ ratios and positive angles of attack, the leading edge vortex caused leading edge separation and a shift of the stagnation point back to the center of the duct. At $\frac{q}{P_b}$ ratios about equal to and greater than 1 the front curtain washed back making the jet appear similar to a jet flap.

SYMBOLS

S - maximum planform area, ft^2

$\bar{c}$ - mean aerodynamic chord of basic P-GEM model

q_∞ - free stream dynamic pressure, $lbs/_{ft^2}$

V_∞ - free stream velocity, ft/sec

L_t - total lift, lbs

D_t - total drag, lbs

M_j - jet mass flow, slugs/sec

V_j - jet velocity at nozzle exit plane assuming isentropic expansion, ft/sec

M - moment about 50% chord of basic P-GEM model, ft. lbs.

C_L - lift coefficient, $\frac{L_t}{q_\infty S}$

C_D - drag coefficient, $\frac{D_t}{q_\infty S}$

C_M - moment coefficient, about 50% chord of basic P-GEM model $\frac{M}{q_\infty S \bar{c}}$

C_μ - jet momentum (blowing) coefficient, $\frac{M_j V_j}{q_\infty S}$ (of circular planform only)

P_b - base pressure (gage), lbs/ft^2

h - height of center of base above ground, inches

h_s - height with forward motion, inches

h_o - hovering height, inches

α - angle of attack, degrees

α_s - pitch trim angle, degrees

δ_t - tail deflection, degrees

D - diameter of circular planform, inches

W - weight, lbs

TABLE OF CONTENTS

		Page
I.	Introduction	1
II.	Description of Model and Test Facilities	
	A. Wind Tunnel Study	3
	B. Free Flight Simulation	4
	C. Smoke Studies	4
III.	Results and Discussions	
	A. Wind Tunnel Studies	5
	B. Simulated Flight	10
	C. Smoke Visualization Studies	11
IV.	Conclusions	15
V.	References	17
	Figures	
	Distribution List	
	Abstract Cards	

I. INTRODUCTION

A circular GEM such as the P-GEM is usually loaded so as to have its center of gravity at the 50 percent chord point so as to be balanced in ground effect. Unfortunately, in forward flight it is desired to have the center of gravity at the aerodynamic center which is located about 25 percent of the mean aerodynamic chord. If the weight is still balanced at the 50 percent chord a nose-up moment will increase with speed. Unless very large control forces are available to balance the nose-up moment or to allow an initial loading forward of the center point, the machine will at some speed run out of control and nose-up. A slight nose-up at this point will give greater lift forward of the center of gravity giving an increasing unstable nose-up attitude. Fortunately, when this maneuver was inadvertently carried out on the P-GEM it was found that the speed dropped rapidly enough with the nose-up attitude so that no damage was done.

To avoid this limitation on speed it was thought that some aerodynamic surfaces such as a tail or swept wing might be placed so as to move the flying aerodynamic center aft to the center of the circle. Any non-blowing surface located aft of the center would help, but it was thought that a high tail or swept wings would be the most interesting to test since the tail would be the more convenient and the wings might give increased aspect ratio. Thus the wind tunnel section of the report is concerned with winged and tailed configurations of a low powered P-GEM model.

Because of the stability problem associated with ground effect machines such as the P-GEM, little is known of their forward flight characteristics at the higher ground heights. Also it is a well known fact that at the

higher speeds the front curtain finally washes back changing the entire nature of lift augmentation due to the ground proximity. Conditions for the turning back of the front curtain are not yet completely established. The last part of this report deals with a simple experiment designed to visualize the washing back of the front curtain on a model of the P-GEM by use of smoke techniques. Flight at the higher altitiudes at speeds in which the front curtain washes back defines the flight regime in which GEMs will have to fly if their performance is to be improved substantially.

Early observations of the P-GEM and in general most GEMs of circular planform revealed that the machines become more stable with forward speed below the regime in which aerodynamic forces predominate. Some results of this report and many others indicate that this stability increase is due mainly to a loss in altitude with forward flight. The flight simulation studies presented in this report investigate the nature of this height decrease with velocity and shed more light on the performance and stability characteristics of GEMs in general.

It is stressed here that the wind tunnel and flight simulation studies were designed to investigate separate problems. No attempt was made to correlate the two studies since the jet momentum coefficient used in the wind tunnel investigations was much lower than those deemed necessary for the Long Track studies.

II. DESCRIPTION OF MODELS AND TEST FACILITIES

A. Wind Tunnel Study

The basic model used in this investigation was a $\frac{1}{12}$ scale approximation of the original P-GEM. A two view schematic drawing of the model is presented in Figure 1. Blowing through the peripherial nozzle was accomplished by use of a D.C. servomotor which drove a four inch diameter fan at 10,000 r.p.m. Input power to the servomotor was about 1/6 horsepower. Separate studies were also made of the basic P-GEM model with non-blowing wings attached in two positions and also with a tail assembly. In the first case two NACA 65_3 - 418 wings were first attached to the perimeter of the model at the 50% chord location, and secondly they were rotated 45° aft of the model's center-line. In both cases the wings were set at zero incidence and the bottom surface of the wings were flush with the base of the model. Each wing had a span of 8 inches and a chord of 4 inches. Drawings of these configurations showing the wing locations are presented in Figure 2. In the second case the basic model was outfitted with a 54 square inch tail supported by two vertical fins. Two pins at the quarter chord attached the tail to the vertical fins so that tail incidence could be varied for control purposes. A drawing of this configuration is presented in Figure 3, and photographs of all four configurations are presented in Figure 4. The wind tunnel used was the Princeton Student Wind Tunnel. The test section is two feet high by three feet wide by four feet long. A three by four foot conventional ground board suspended from the tunnel ceiling was used to simulate the ground proximity. The leading edge of the ground board was placed 8 inches ahead of the nose of the model to insure horizontal flow at the model. Measurements of lift, drag and pitching moment were obtained by use of a three component strain gage setup.

B. Free Flight Simulation

A 1/5 scale approximate model of the P-GEM was tested in the Princeton Forward Flight Facility (Long Track). The balsa model was powered by a 2 horsepower, 3 phase electric motor which drove a 1 foot diameter single bladed prop. To insure symmetrical blowing the model was internally segmented into thirty-two radial ducts which carried flow from the center duct to the peripheral nozzle. A schematic drawing of the model showing pertinent dimensions is shown in Figure 5A. A complete description of the Long Track Facility can be found in Reference 1. Briefly, forward flight was simulated by use of a carriage which drew the model over the concrete floor. The assembly of the carriage permitted height movement restricted to 3½ inches with the minimum usually set 1 inch above the ground; also pitch movement was restricted to $\pm 5^{o}$. These restrictions on height and pitch were made to prevent structural damage to the model. A photograph of the model mounted on the carriage is presented in Figure 5B.

C. Smoke Studies

Smoke visualization studies using the P-GEM model, the swept wing configuration, and the tailed configuration were made in the Princeton Three Dimensional Smoke Tunnel. The tunnel is glass enclosed on three sides to permit easy accessibility for lighting and photography. Internal smoke ducts placed within the models carried smoke to outlets located on the extremities of the models. At times smoke probes were used when additional smoke was necessary for flow visualization. Photographs of the tailed configuration mounted in the tunnel are shown in Figure 15.

III. RESULTS AND DISCUSSION

A. Wind Tunnel Studies

The longitudinal aerodynamic characteristics of the four P-GEM model configurations at various ground heights are presented in Figures 6 to 9. As might be expected, the results show for all configurations, both with and without blowing, an increase in effective aspect ratio as the ground was approached. This increase in effective aspect ratio shows up as a reduction in induced drag coupled with an increase in lift curve slope, which results in higher lift-drag ratios at higher lift coefficients, (see Fig. 6C for a typical example). It is noted that blowing caused a considerable increase in drag. Momentum drag coefficient in this case is approximately .086 which can account for most of this increase. Also blowing may have had some effects on profile drag. Little change is seen in the lift curve slope at zero angle of attack due to blowing. However, in all configurations blowing increased the slope of the lift curves at negative angles of attack. In some cases, particularly the winged configurations, blowing produced slight decreases in lift curve slope at positive angles of attack. As one would expect these effects of blowing are reflected by a general decrease in $^{L}/D$ and an increase in lift coefficient for maximum $^{L}/D$. A comparison of the data for the basic model, presented in Figure 6, with the winged configurations reveals that, as expected, both effective aspect ratio, and consequently, $^{L}/D$ ratio increase with geometric aspect ratio. But, a comparison of Figure 6 with the tailed configuration, presented in Figure 9, shows that the tail also increased effective aspect ratio even though geometric aspect ratio

decreased if we consider tail area is added to wing area. Thus it appears, in this particular case, that the tail together with its supporting vertical fins establishes a biwing and/or boxwing effect which increases effective aspect ratio.

The static longitudinal stability data for all configurations except 45° swept wings shows, with no blowing at positive angles of attack, a stability increase as ground height decreases. The reason for this can be thought of as a restriction of downwash at the trailing edge which occurs at low $^{h}/D$ ratio with positive angles of attack. A more physical picture of this effect may be had by considering it to be an increase in pressures on the aft section of the model base due to the "Ram Effect" of the airflow between the base of the model and the ground. This Ram Effect produces a restoring moment that decreases non-linearly with reduced angle of attack, and is, therefore, a stable contribution to the stability of the models. This view is further supported by the fact that with no blowing the stability at all ground heights is approximately the same at negative angles of attack. Near the ground ($^{h}/D$ = .090) blowing appears to slightly decrease the stability of the basic model and 90° wing configurations at the higher angles of attack. Contrary to this, it seems reasonable to expect at positive angles of attack that the difference in lift augmentation between the front and rear sections of the jet would produce a restoring moment which would increase stability at low $^{h}/D$ ratios. However, smoke visualization studies indicate that the front curtain tucks back under the model at test dynamic to base pressure ratios ($^{q}/Pb > 1$) (see Smoke Studies, part C). If this decrease in stability is correct,

then a plausible conclusion is that this change in the front curtain has something to do with it. This particular effect of blowing, however, can not be detected in the configurations which substantially changed the stability of the basic model. The data of Figures 6 and 7 also show a slight increase of trim angle of attack with increasing $\frac{h}{D}$ ratio and at most a 2^{o} increase in trim angle with blowing.

Figures 7 and 8 show the effect of moving the aerodynamic center back by use of wings. As seen in Figure 7 the small rearward movement of the aerodynamic center by use of wings mounted at the 50% chord location does very little good in improving stability. Figure 8 shows the effect of moving the aerodynamic center back even further by use of swept wings mounted 45^{o} aft of the model centerline. As can be seen, this configuration realizes a substantial increase in stability at low positive and negative angles of attack. Unfortunately, when mounted in this position the root sections of the wings are screened from the flow by the circular body of the model at the higher angles of attack. Consequently, there is little improvement to stability in this angle of attack region. This situation could probably be remedied by locating the root sections of the wings further forward on the model or by fairing of the main circular body. Finally, as seen in Figure 9, the addition of the 54 square inch tail also increases stability substantially. In fact, within ground effect stability is achieved at positive angles of attack with marginal stability at negative angles of attack. Furthermore, marginal stability also is achieved out of ground effect. Figure 9 also shows the control moments possible with tail deflection which suggests that a tail could greatly enhance the longitudinal control of GEMs. It appears then on the basis of these results, that

despite their awkwardness and increase to bulk size, either a tail or swept wings would be powerful tools for abetting the static longitudinal stability of GEMs such as the P-GEM within and out of ground effect.

The data of Figure 10 represents the aerodynamic characteristics of the P-GEM model with first the front half and then the back half of the peripheral jet closed. In these tests the tunnel was run at a dynamic pressure of 4 lbs per sq. ft. and smoke studies indicated that the forward curtain washed back with front blowing. It is interesting to compare the lift and drag produced in both cases. Back blowing produces much higher lift coefficients than front blowing; and due to jet momentum thrust direction and possible increases in friction and form drag the profile and minimum drag coefficients are higher in back blowing. Also judging from lift curve slope and drag curve shape there appears to be no differences in induced drag at the higher $^{h}/D$ ratios. Consequently, front blowing produces higher $^{L}/D$ ratios and maximum $^{L}/D$ at these $^{h}/D$ ratios. However, at the lowest ground height ($^{h}/D = .090$) the lift curve slope is greater and induced drag is less in back blowing. As a result of this, $\frac{L}{D}$ for back blowing surpasses $\frac{L}{D}$ for front blowing at a lift coefficient of .80, the reason for it being somewhat unclear. Obviously, there must be an abnormal change in the flow pattern due to the proximity of the ground; although smoke studies didn't clarify this point. However, it was noted through smoke visualization of the airflow that in front blowing the curtain adheres somewhat to the base of the model as in a coanda effect; this may explain all or part of the loss in jet induced pressure lift with front blowing. It is also interesting to note that both front and back blowing produce higher $^{L}/D$ ratios than full blowing does, and this suggests there may be an advantage in shutting off

part of the jet once the front curtain washes back in forward flight. Finally, if we view the equilibrium conditions produced in each case from the standpoint of using differential blowing for control purposes, we see that an incompatible situation exists. For control purposes front blowing is usually used to produce nose up attitudes, but in this case equilibrium occurs at negative angles of attack with front blowing. Also back blowing is usually used to produce nose down attitudes but equilibrium occurs at positive angles of attack with back blowing. Possibly because much smaller sections of the front and rear slots are opened and closed to provide longitudinal control in GEMs such as the P-GEM this phenomenon has not yet been experienced. However, this study indicates the need of further investigations into the change in trim conditions with varying front and rear slot closure, expecially at higher blowing coefficients than used in these tests and with the front curtain washed back. Unfortunately, the exact value of C_μ used in this blowing series was unknown, but if we assume that no losses occur with slot closure C_μ would be .04.

Figure 11 shows the change in lift and drag coefficients with jet momentum (blowing) coefficient. The jet momentum was determined by ascertaining the mass flow through the nozzle by exhausting the jet into a plastic bag of known volume. The variation in C_μ was achieved by varying tunnel velocity keeping jet momentum essentially constant. As seen in the Figure the change in C_L is an increasing function of C_μ and aspect ratio, but a decreasing function of ground height; whereas the change in C_D appears to be primarily an increasing function of C_μ with only slight variation with aspect ratio and ground height.

B. Simulated Flight

Both pitch fixed and pitch free runs were made at various velocities and model power settings. The pitch fixed runs were made to determine the nature of height decay with respect to weight to jet momentum ratio and velocity; while the pitch free runs were made to determine the variation of pitch trim with flying height. The results are presented in Figure 12.

Figure 12, graph A shows the decay in flying height versus velocity at various values of the $\frac{W}{MjVj}$ ratio with pitch set at zero. In these runs the model was symmetrically loaded with four and eight pounds of ballast to vary weight, and momentum thrust was varied by changing power input to the model. As expected hovering and flying heights increased with decreasing $\frac{W}{MjVj}$ ratio and decreased with increasing velocity up to about 30 ft/sec. However, it was noted that a height variation greater than expected for normal error (about $\pm$ 10% hovering height) occurred for all model weights at speeds in excess of 30 ft/sec. This lack of height stability was less pronounced with increasing model weight; the three wing loadings used were 1.34 $^{\#}/ft^2$, 1.65 $^{\#}/ft^2$ and 1.97 $^{\#}/ft^2$. Since this height instability seemed to start at dynamic pressures between .8 $^{\#}/ft^2$ and 1.6 $^{\#}/ft^2$, it is reasonable to assume the phenomenon was due to the development of aerodynamic lift nearly sufficient for take-off. This is further indicated by the fact that the flying heights tend to be higher at the top speeds. Unfortunately, due to model structural limitations higher speeds were avoided and so this study only touched lightly upon the take-off phenomena. But it does suggest an excellent field for future investigations.

Figure 12 graph A is cross plotted in graph B to more plainly show the variation of flying height with $\frac{W}{MjVj}$ ratio at constant velocity. This plot shows greater losses in flying height with velocity as $\frac{W}{MjVj}$ decreases. However, as seen in graph C the percentage loss in height due to forward motion is nearly constant with $\frac{W}{MjVj}$ being a function of velocity until take-off speeds are approached.

Results of the pitch trim studies, shown in Figure 12 graph D, show an increase in trim angle with increasing flying height (i.e. decreasing stability). This same result was also found in wind tunnel studies, (see Wind Tunnel Studies, part A). Observations revealed that the model became unstable in pitch at heights in excess of 3 inches (height to diameter about .06). Pitch stops were placed at $\pm 5^{o}$ to prevent the model from hitting the ground. A major point of interest is that pitch instability occurred in hover at about the same altitude as with forward flight. This suggests that the increases in stability with forward flight experienced in GEMs such as the P-GEM may be largely due to decreases in height. However, wind tunnel studies show that other factors may be involved particularly when differential blowing is used for tilting the machine to obtain a thrust vector.

It is to be noted that during these runs $C\mu$ varied from .26 to 5.6 which was considerably higher than the $C\mu$ of .04 used in the wind tunnel studies.

C. Smoke Visualization Studies

Smoke visualization studies were made to observe the streamline flow and vortex formation with and without blowing. The models used in these tests were the basic P-GEM model, the winged configuration, and the tailed configuration.

Figure 13 shows the observed topside flow with and without blowing. It will be noted that with blowing the streamlines are pulled inboard towards the rear of the model. (In particular note the two streamlines directly behind the duct.) The plausible reason for this is that flow is aspired inboard behind the duct to make up for the flow ingested into the sink; also, as will be seen later, blowing increases the tip vortex which may further contribute to this. This same flow pattern also appears to be dominant in tuft studies of the full scale P-GEM, (see Reference 2). To date, drag components have not been completely separated in drag measurements so it is difficult to tell whether this altered flow is beneficial to parasite drag. However, it appears that blowing produces a smoother flow which might cause a reduction in parasite drag.

Figure 14 is a systematic study of the behavior of the front jet curtain with increasing dynamic to base pressure ratios. In these tests momentum thrust was held constant and q/P_b ratio was set by varying tunnel velocity. This method most realistically simulates the increase q/P_b ratio as full scale machines accelerate. It was found at q/P_b ratios equal to and less than .8 that the front curtain rolled up into a horseshoe type vortex system that extended around the front perimeter of the model blending with and strengthening the familiar trailing vortices at the wing tips. A photograph of this vortex system and a comparative photograph with no blowing appear in Figure 15. Particular attention was paid to the vortex formation at the nose of the model, and a detailed photograph of this nose vortex appears in Figure 16. The nature of this vortex seems to depend on both q/P_b ratio and angle of attack. The vortex grows looser and slower as q/P_b decreases and also as angle of attack increases. In fact at the

higher angles of attack with q/P_b set at .50 the vortex causes the flow to separate from the nose of the model, shifting the stagnation point back to the center of the duct. With q/P_b equal to .80 the size of the vortex becomes smaller at each angle of attack, and although it is difficult to see in the photographs, the front curtain still washes forward slightly at zero and negative angles of attack. Finally as dynamic pressure exceeds base pressure the front curtain washes back in a jet flap fashion. Although its not pictorially presented in this report, trial studies at various ground heights reasonably close to the ground produced simular results. Under some conditions the curtain may have washed back sooner than others, possibly at q/P_b ratios slightly less than 1. It seems that the curtain is less inclined to wash back at the higher angles of attack. This implies that the radius of curvature and the number of degrees the flow has to be turned may be factors involved. Also the strength of the vortex governed by momentum thrust (MjVj) as well as jet width and angie may be other factors involved. The possible influence of these factors should be studied on a more sophisticated model.

It appears that snubbing the nose, adding wing fences, and especially adding wing tip plates would cut down the downwash from the curtain vortex system. However it is recommended that measurements should be taken to verify this.

Observations made of the swept wing configuration show that due to their rearward outboard position near the base of the model a major portion of the wings are in a upwash region. Without blowing this upwash is due to the normal tip vortex of the circular portion of the model when positive

lift is generated; while with blowing this upwash is further enhanced by the curtain vortex system mentioned earlier. Observations made of the tailed configuration show that the tail operates in a region of slight downwash. Therefore, small swept wings designed to operate in this upwash region may improve stability more than a comparable sized tail.

IV. CONCLUSIONS

1. Both with and without blowing effective aspect ratio increases as the ground is approached.
2. Blowing increases the drag considerably. Most of this increase can be attributed to momentum drag and possibly a slight increase in profile drag.
3. A proper tail assembly designed to form a biwing combination with the main circular body slightly increases effective aspect ratio, while considerably aiding longitudinal stability.
4. Non-blowing surfaces such as properly located swept wings can increase both aspect ratio and longitudinal stability significantly due to a planform change and their ability to operate in a upwash region caused by the curtain vortex.
5. 180^{o} front blowing and 180^{o} back blowing produce higher $^{L}/_{D}$ ratios than full blowing does. This suggests there may be an advantage in shutting off part of the jet once the front curtain washes back in forward flight.
6. Negative trim angles occur with 180^{o} front blowing, and positive trim angles occur with 180^{o} back blowing. This suggests that control reversal may occur when this amount of differential blowing is used for control purposes, and, therefore, indicates the need for further investigations into the change in trim conditions with varying degrees of front and rear slot closure.
7. At speeds in excess of 30 ft/sec the long track model begins to transist into a take-off. During this transition the model is much less stable in height than at lower speeds.

8. The percentage loss in flying height due to forward motion is nearly constant with $\frac{W}{MjVj}$ ratio being dominantly a function of velocity until take-off speeds are approached.

9. Pitch trim angle increases positively with increasing flying height, and pitch instability occurs in hover at about the same altitude as with forward flight.

10. With blowing the streamlines are pulled inboard towards the rear of the model. The plausible reason for this is that flow is aspired inboard behind the duct to make up for the flow ingested into the sink, and blowing increases the tip vortex which also rotates the top streamlines inboard.

11. At q/P_b ratios equal to or less than .8 and at low ground heights the front curtain rolls up to a horseshoe type vortex system extending around the front perimeter of the model. At q/P_b ratios about equal to and greater than 1 the front curtain washes back under the base of the model.

V. REFERENCES

1. Martinez, E., "A New Facility for the Study of Aircraft Dynamics", Princeton University Aeronautical Engineering Report No. 532, July 1961.

2. Sweeney, T. E. and Nixon, W. B., "Some Notes on the P-GEM", Princeton University Aeronautical Engineering Report No. 537, January 1961.

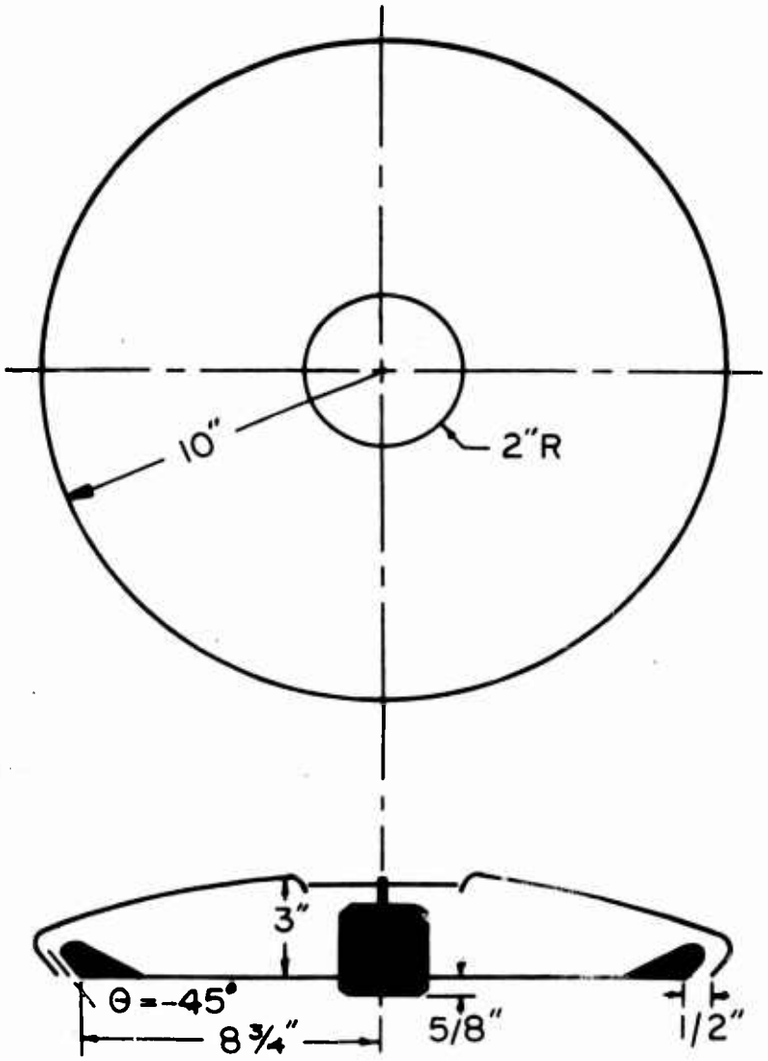

SCHEMATIC LAYOUT AND BASIC DIMENSIONS
OF 1/12 SCALE P-GEM MODEL

FIG. 1

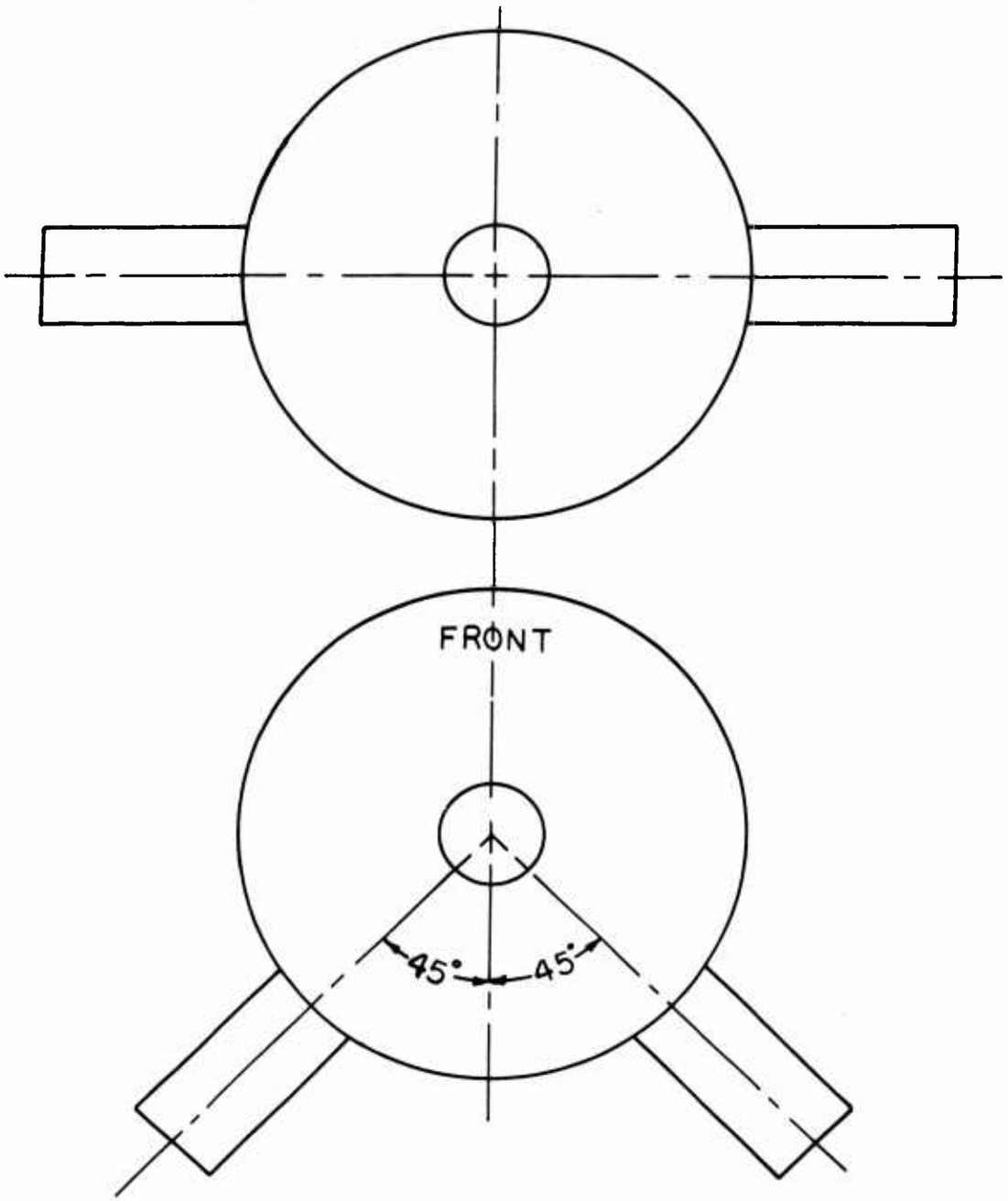

P-GEM MODEL WITH TWO 4"x8" WINGS ATTACHED
IN THE 90° AND 45° POSITIONS

FIG. 2

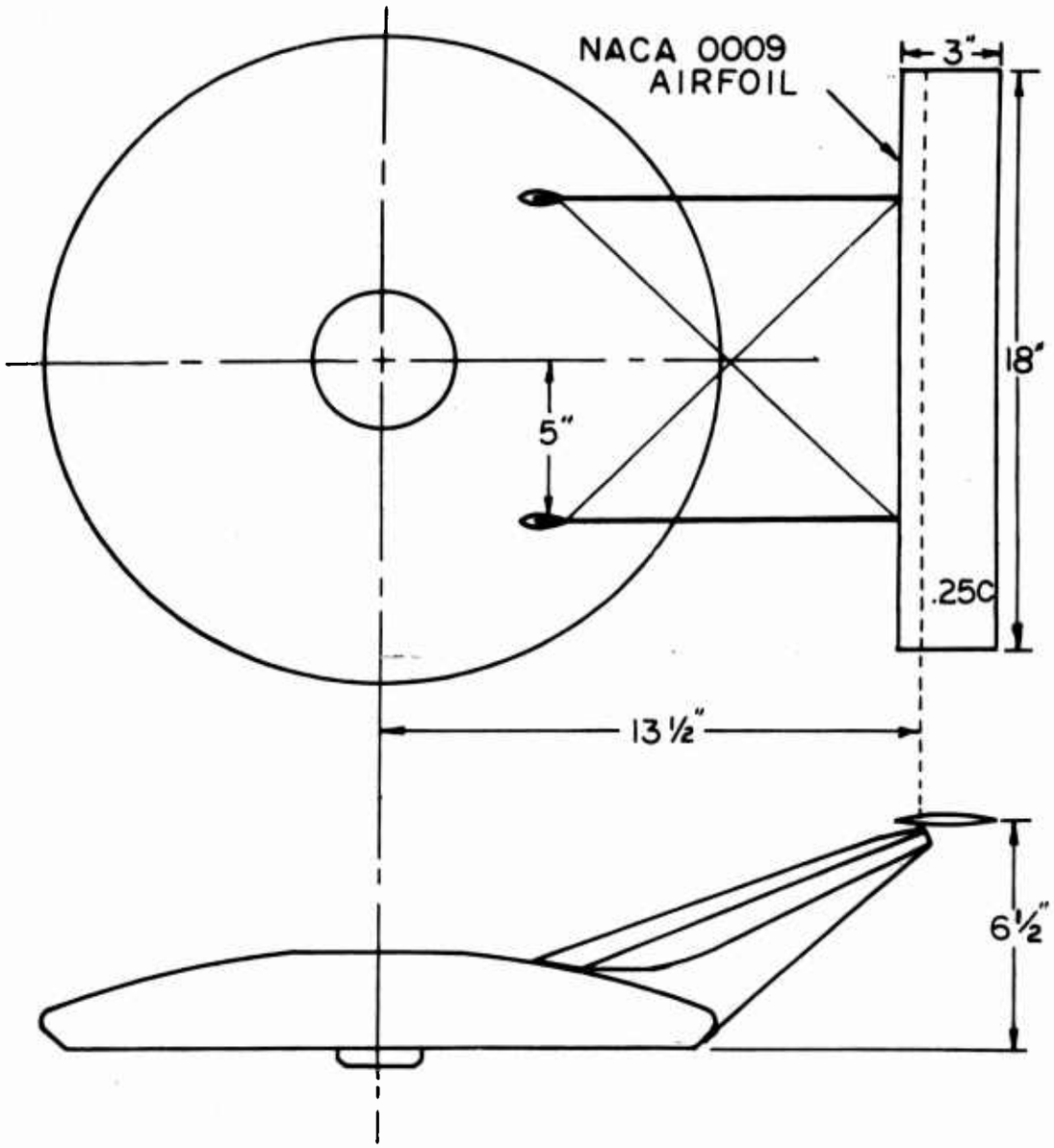

P-GEM MODEL SHOWING TAIL ASSEMBLY

FIG. 3

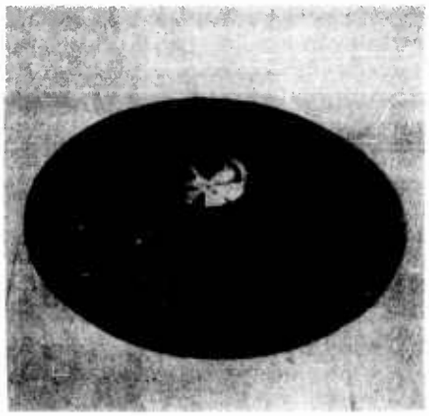

P-GEM MODEL

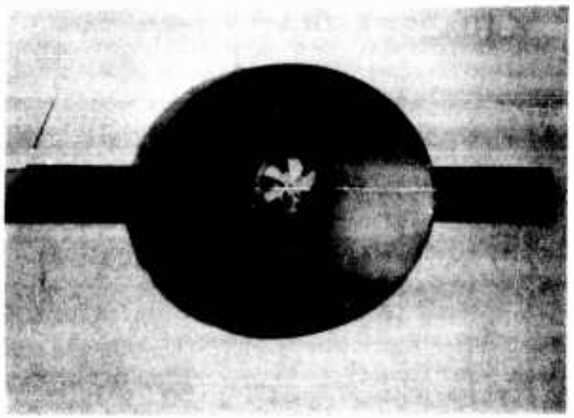

WITH 90° WINGS

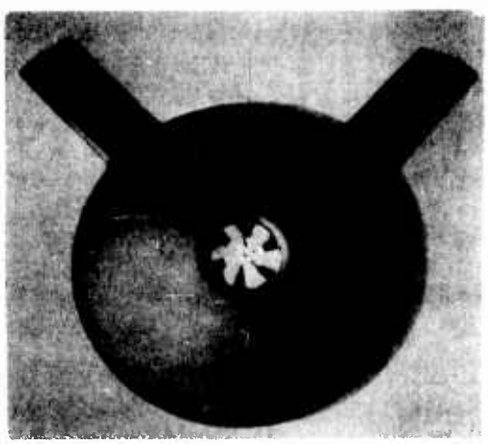

WITH 45° WINGS

WITH TAIL ASSEMBLY

WIND TUNNEL MODELS

FIG. 4

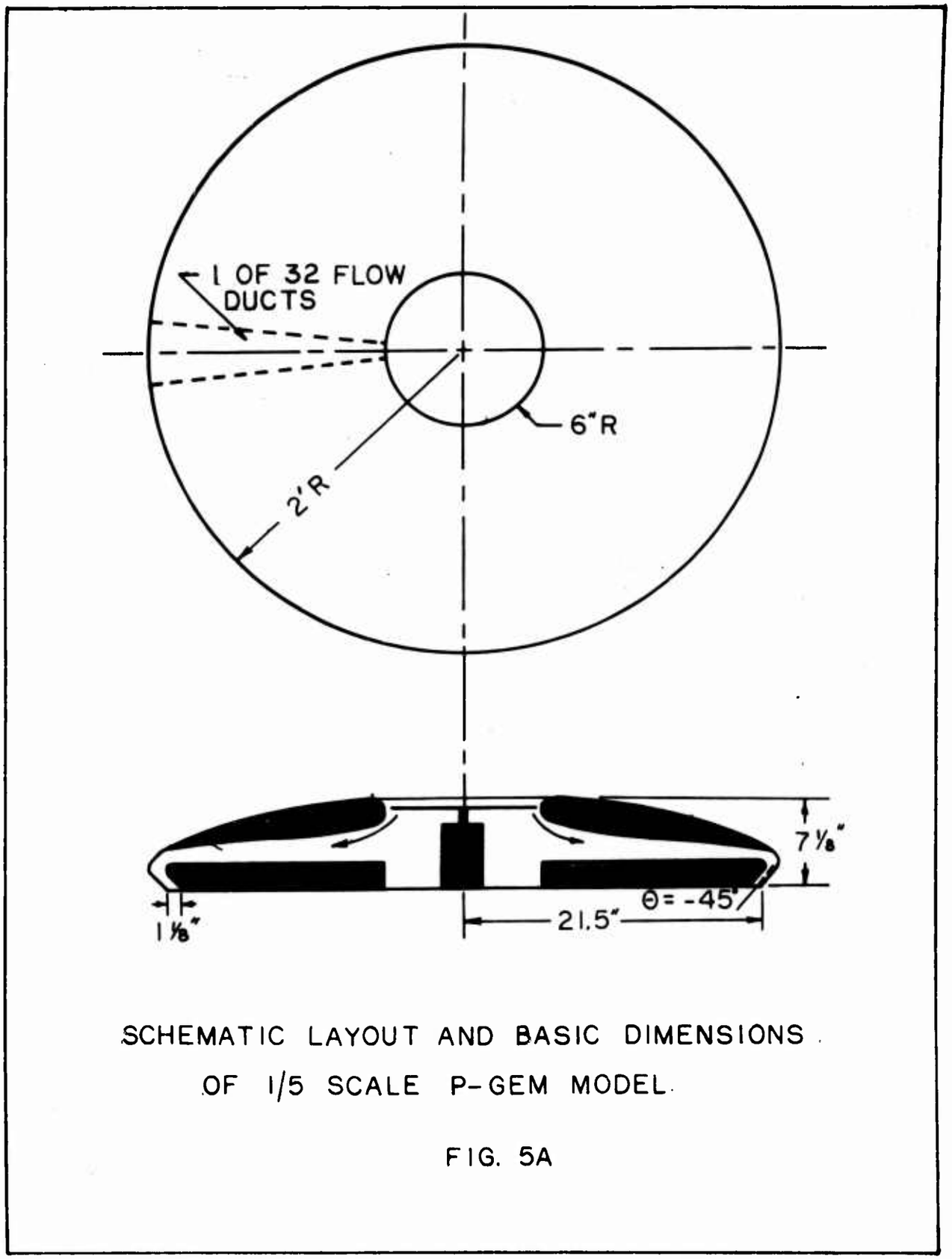

SCHEMATIC LAYOUT AND BASIC DIMENSIONS OF 1/5 SCALE P-GEM MODEL

FIG. 5A

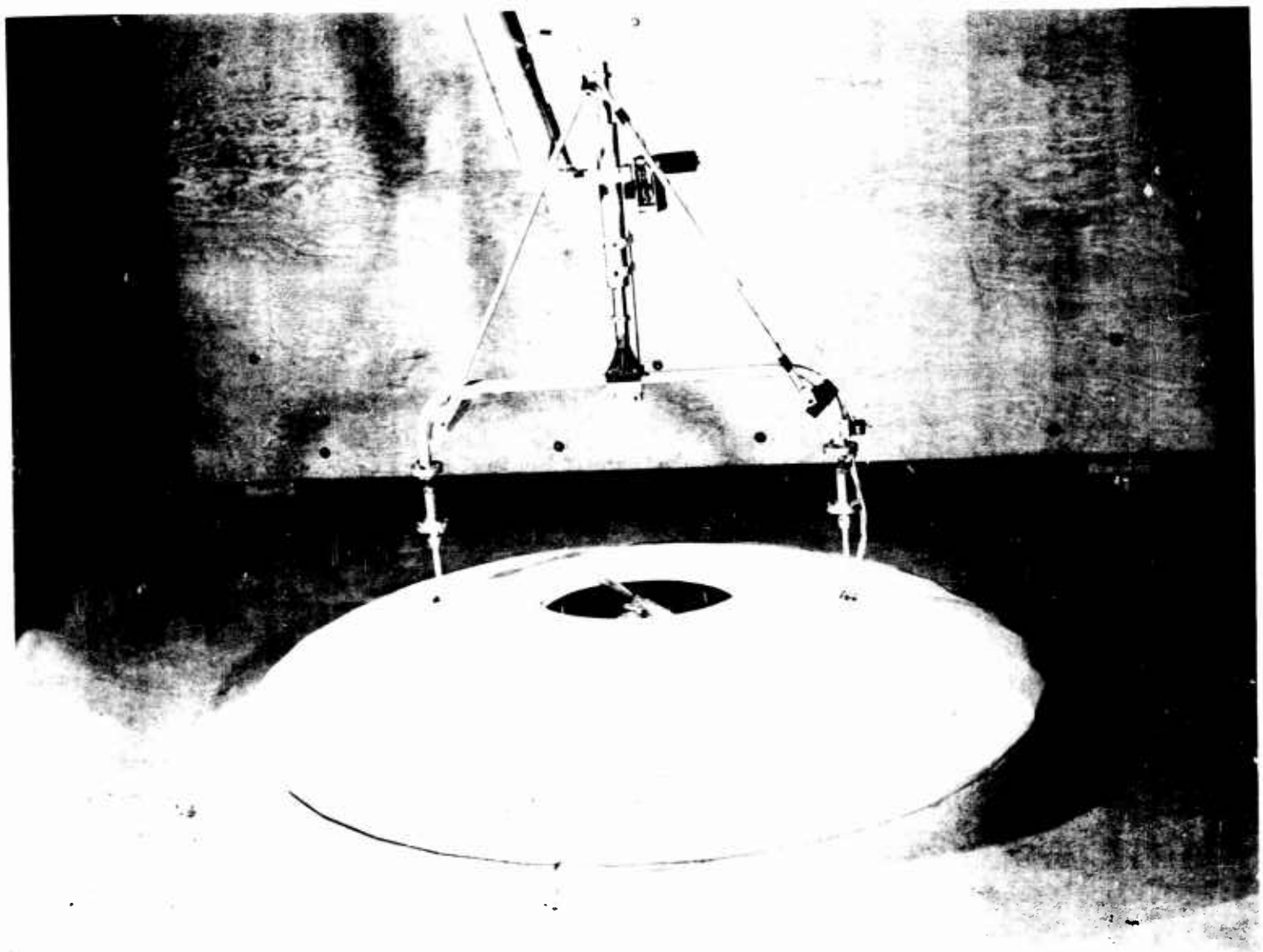

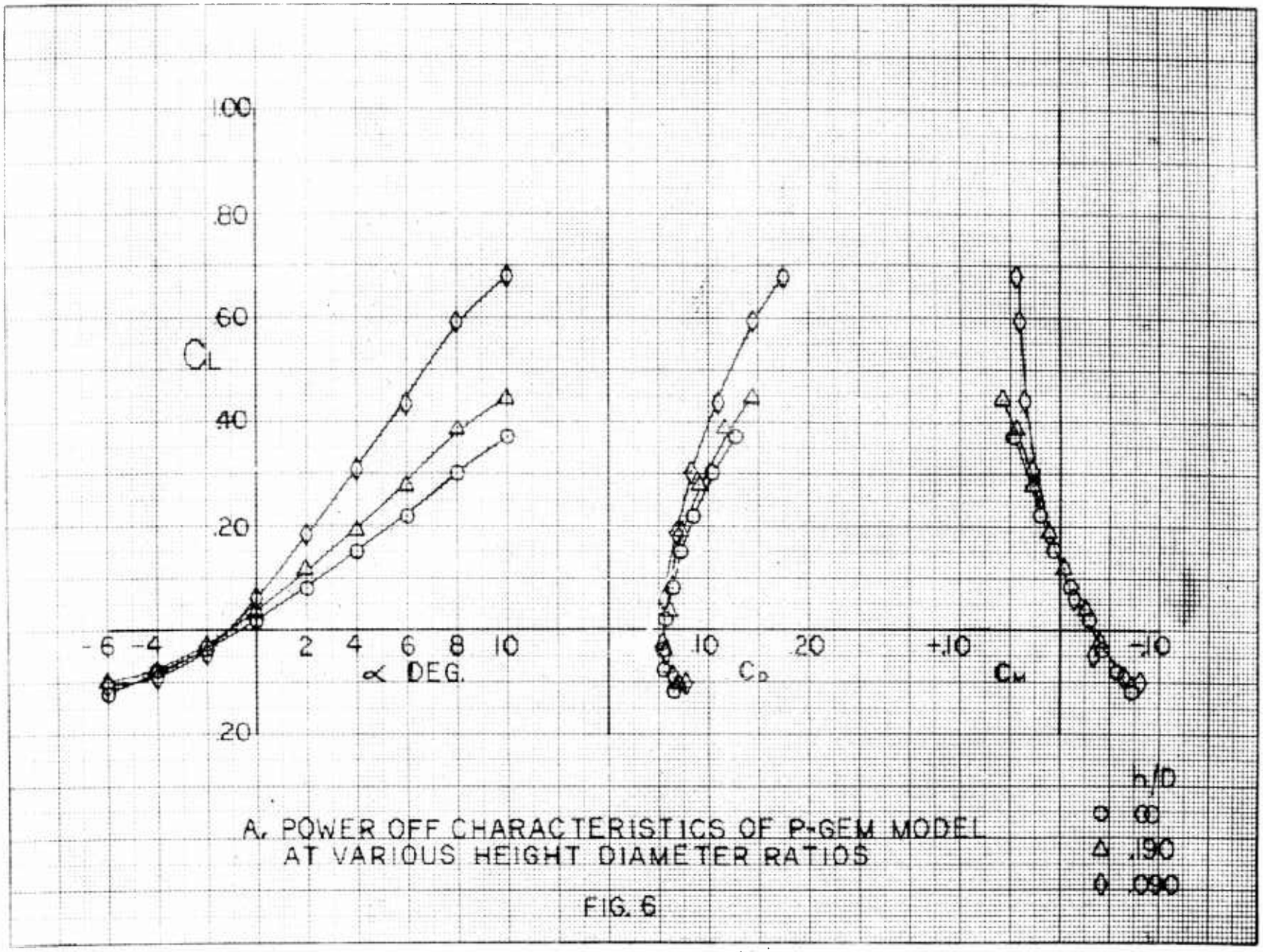

A. POWER OFF CHARACTERISTICS OF P-GEM MODEL AT VARIOUS HEIGHT DIAMETER RATIOS

FIG. 6

K•E 359T 14

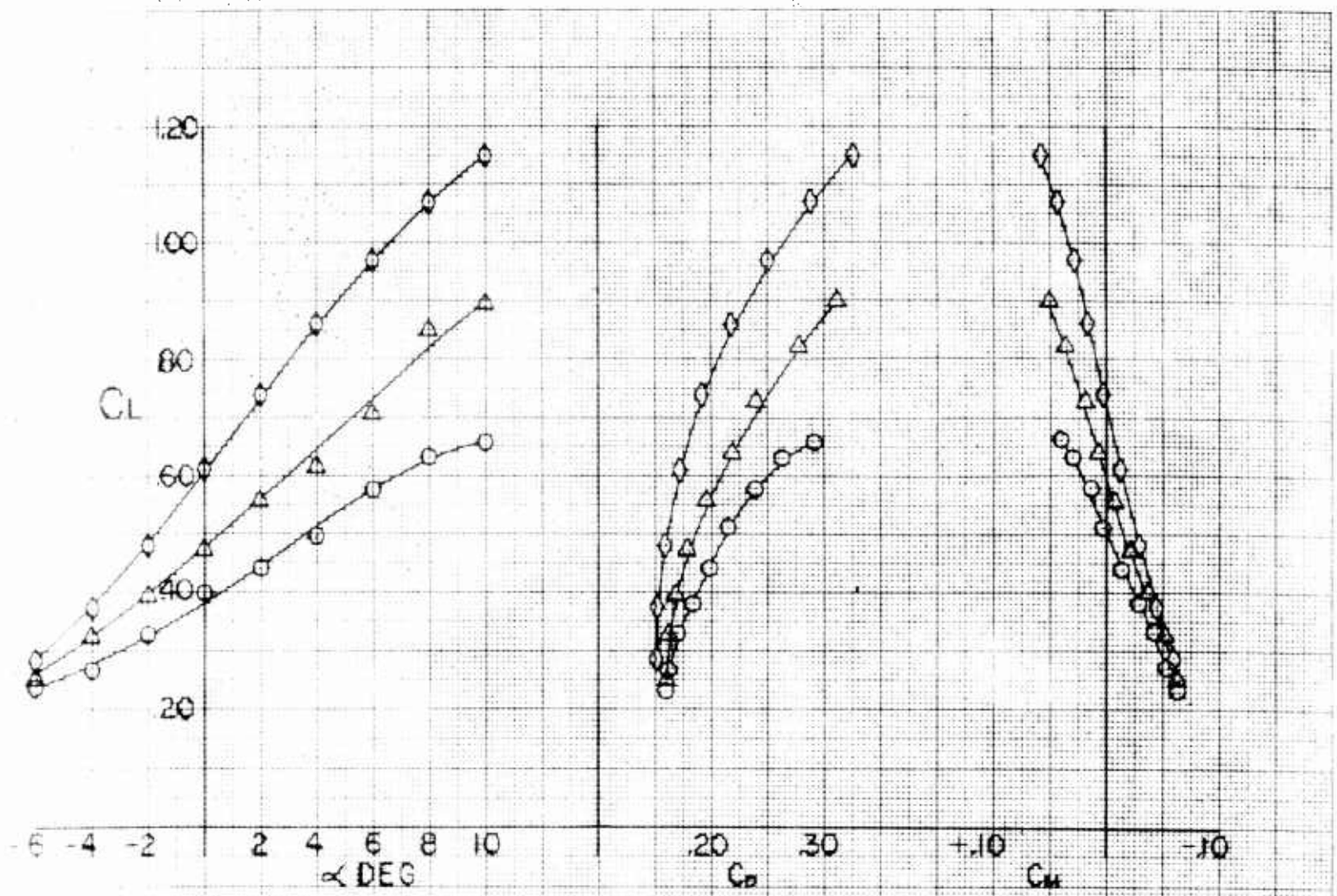

B. POWER ON CHARACTERISTICS OF P-GEM MODEL AT VARIOUS HEIGHT DIAMETER RATIOS (C_μ=.04)

FIG. 6 CONTINUED

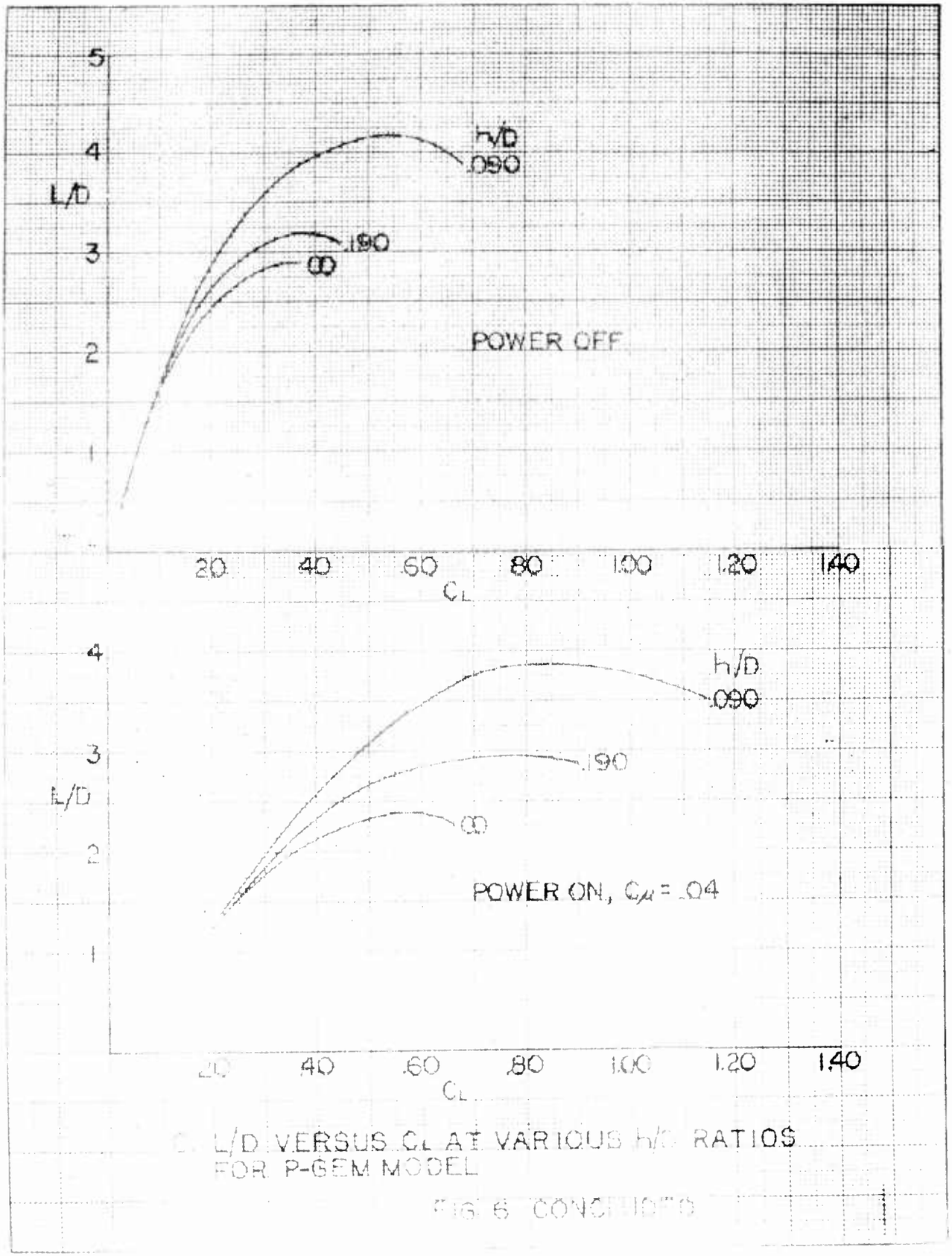

L/D VERSUS C_L AT VARIOUS h/D RATIOS FOR P-GEM MODEL

FIG 6 CONCLUDED

K·E 10 X 10 TO THE CM. KEUFFEL & ESSER CO. ALBANENE 359T-14 MADE IN U.S.A.

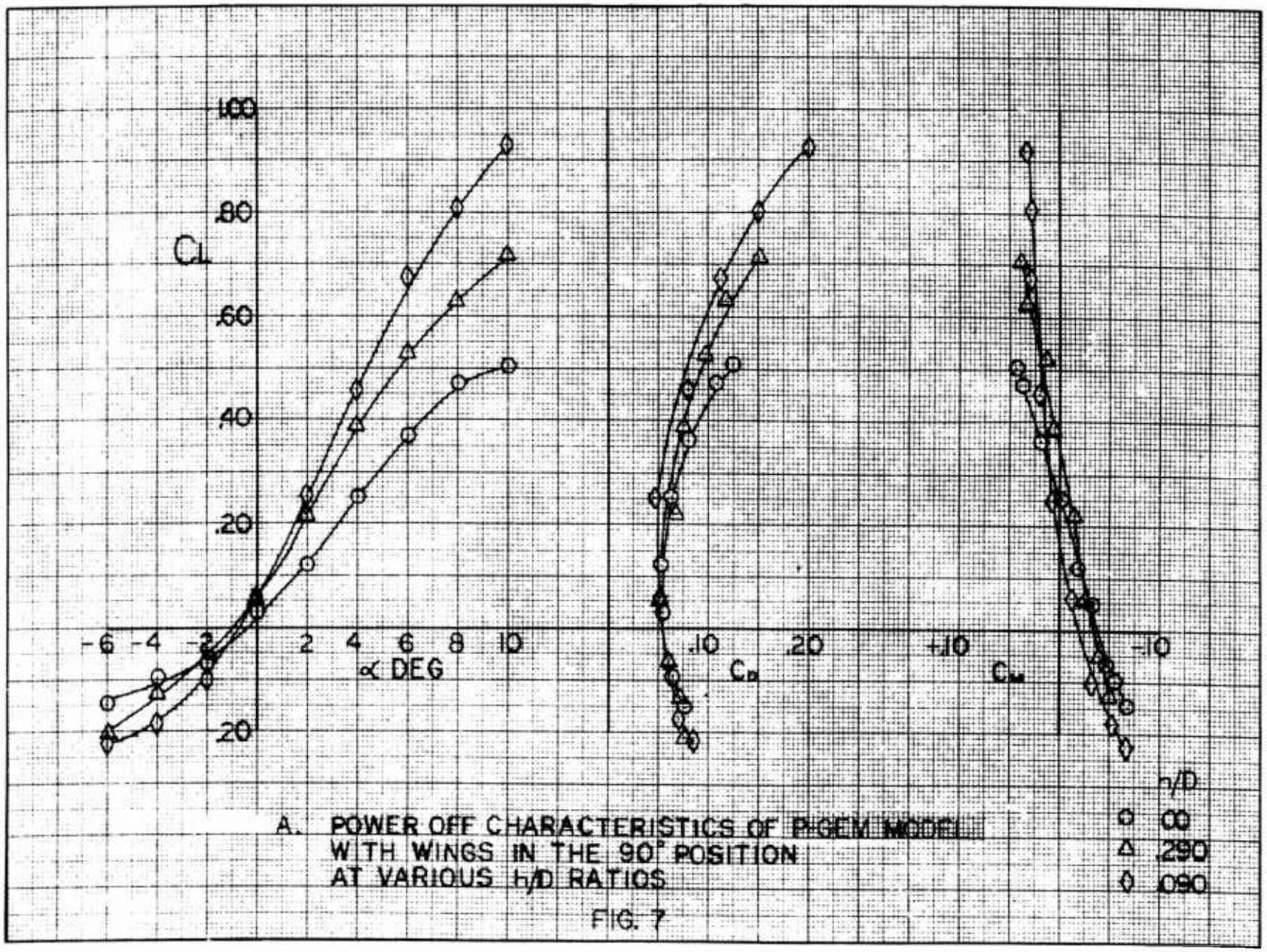

A. POWER OFF CHARACTERISTICS OF P-61M MODEL WITH WINGS IN THE 90° POSITION AT VARIOUS h/D RATIOS

FIG. 7

K&E 10 X 10 TO THE CM 359T-14
KEUFFEL & ESSER CO.

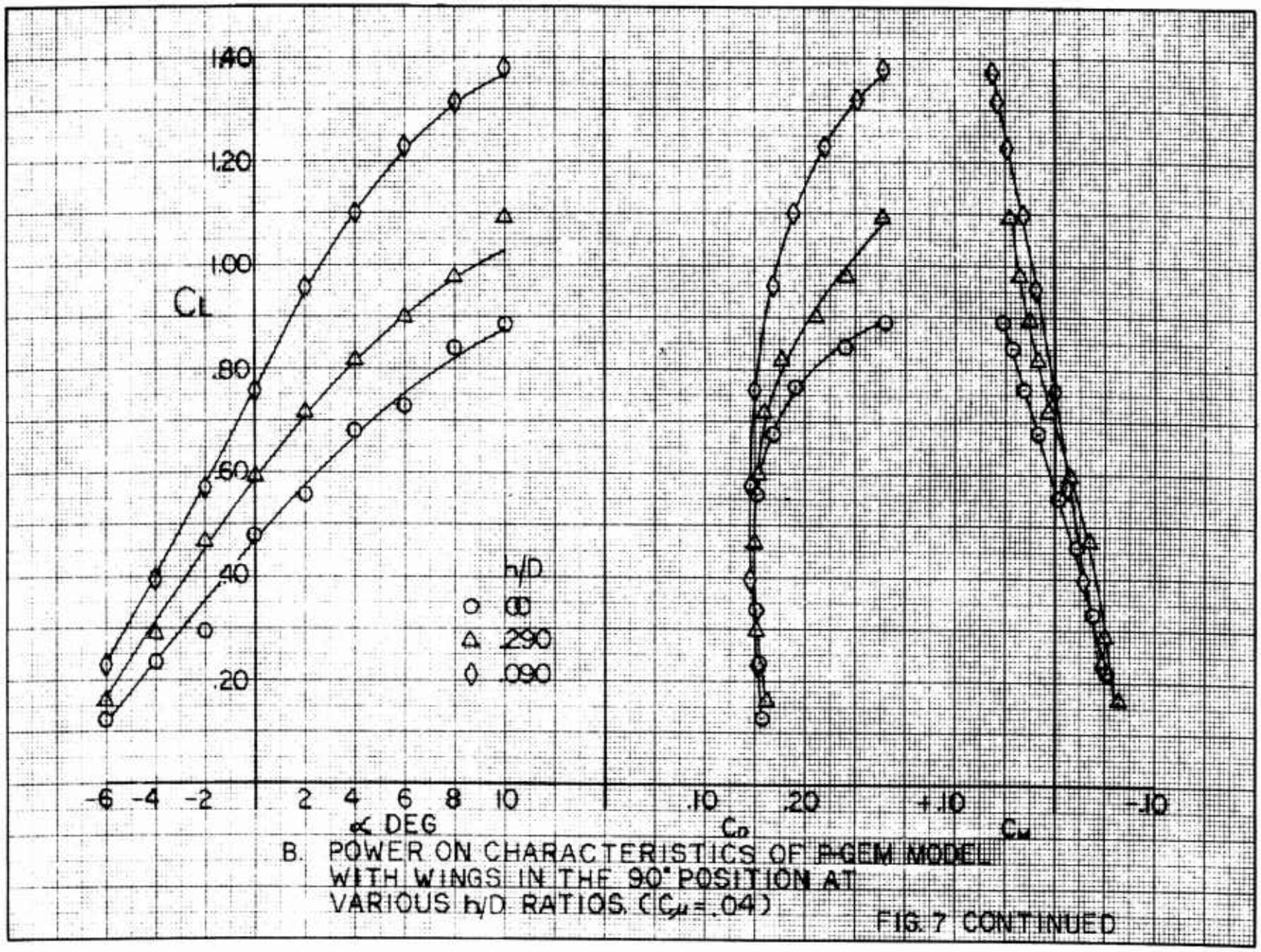

B. POWER ON CHARACTERISTICS OF P-GEM MODEL WITH WINGS IN THE 90° POSITION AT VARIOUS h/D RATIOS. (C_μ = .04)

FIG. 7 CONTINUED

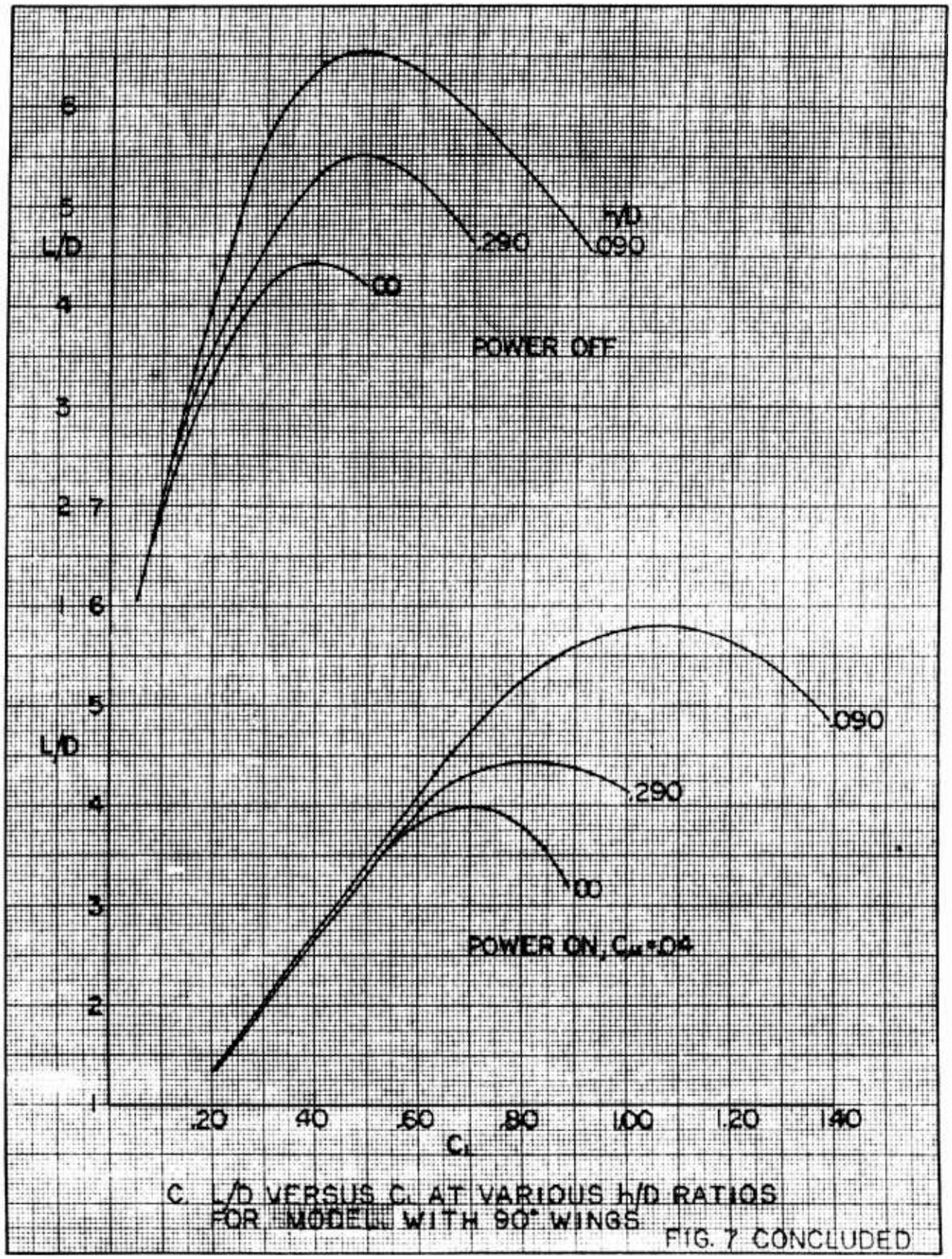

C. L/D VERSUS C_L AT VARIOUS h/D RATIOS FOR MODEL WITH 90° WINGS

FIG. 7 CONCLUDED

K+E 10 X 10 TO THE CM. 359T-14
KEUFFEL & ESSER CO. MADE IN U.S.A.
ALBANENE ®

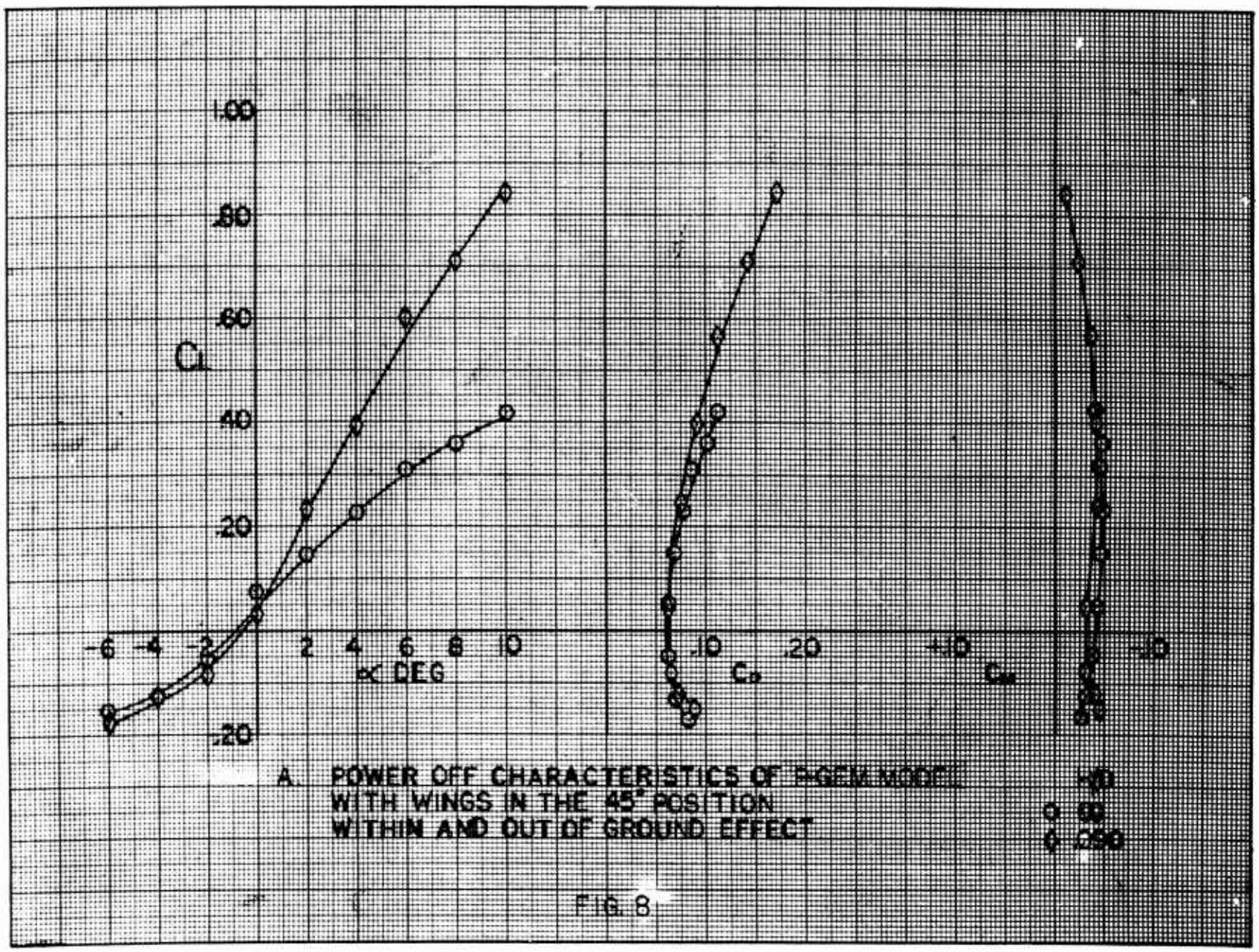

A. POWER OFF CHARACTERISTICS OF 5-GEM MODEL WITH WINGS IN THE 45° POSITION WITHIN AND OUT OF GROUND EFFECT

FIG. 8

K+E 10 X 10 TO THE CM. KEUFFEL & ESSER CO. ALBANENE 359T-14 MADE IN U.S.A.

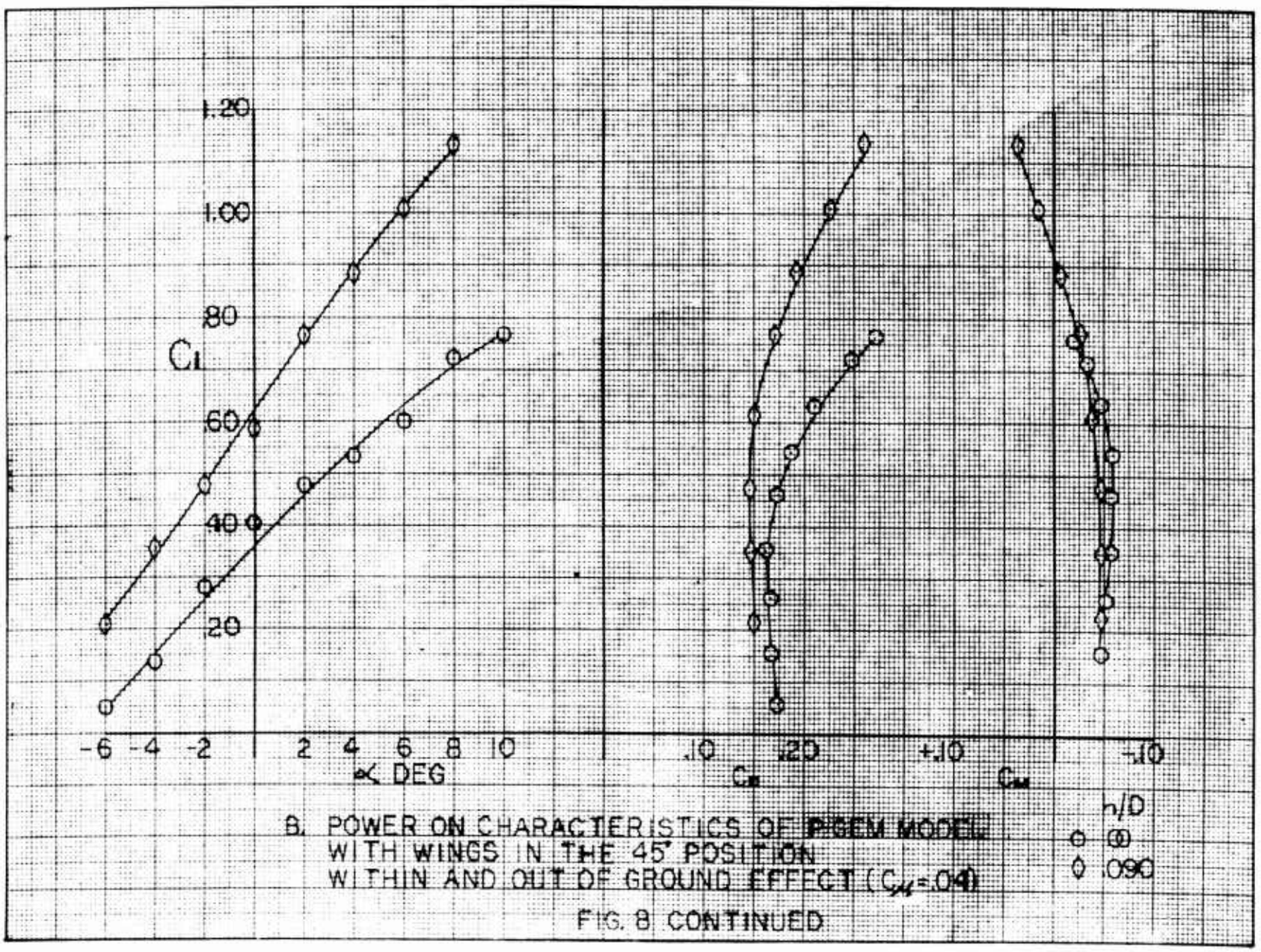

B. POWER ON CHARACTERISTICS OF PGEM MODEL WITH WINGS IN THE 45° POSITION WITHIN AND OUT OF GROUND EFFECT (C_{μ}=.04)

FIG. 8 CONTINUED

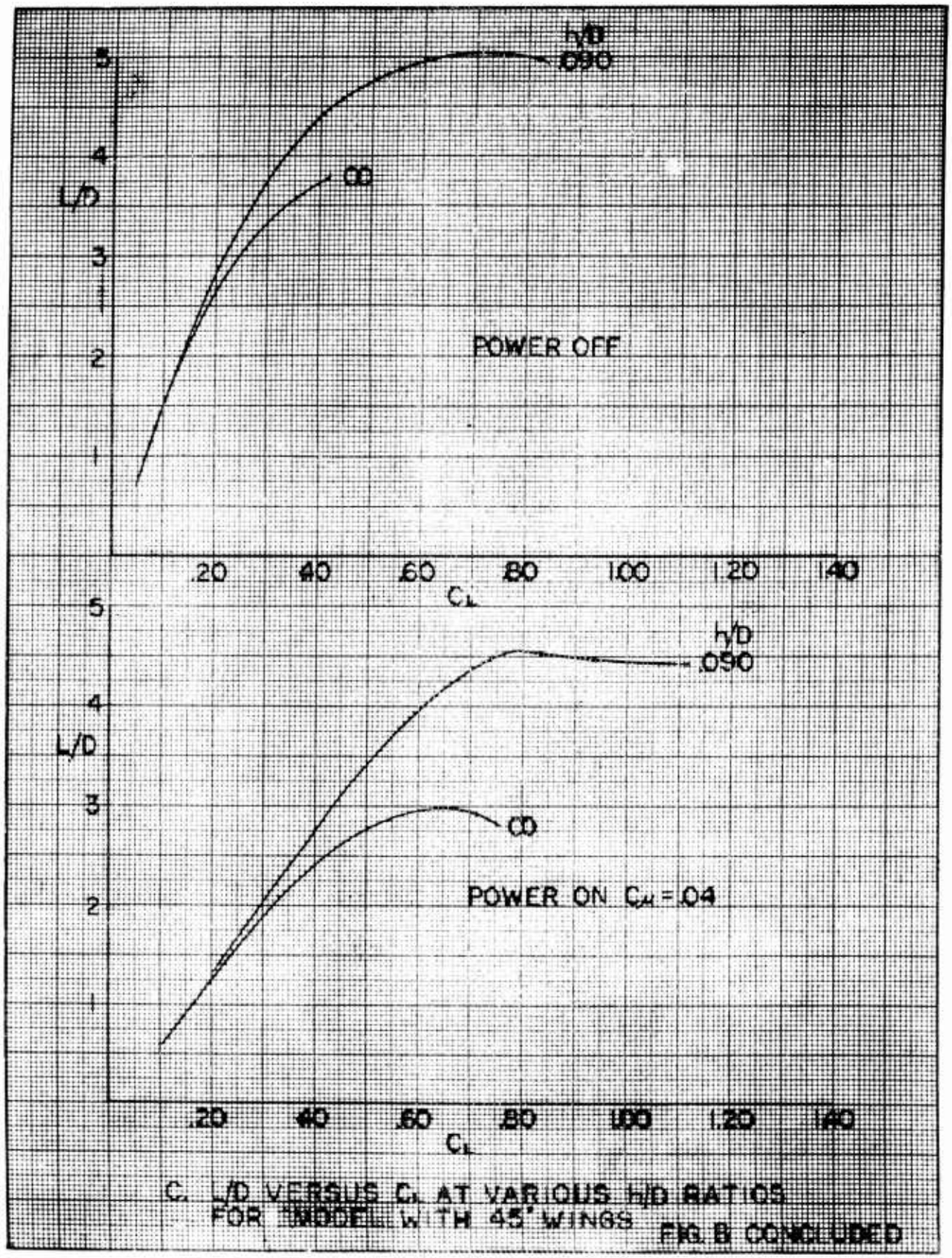

C. L/D VERSUS C_L AT VARIOUS h/D RATIOS FOR MODEL WITH 45° WINGS

FIG. 8 CONCLUDED

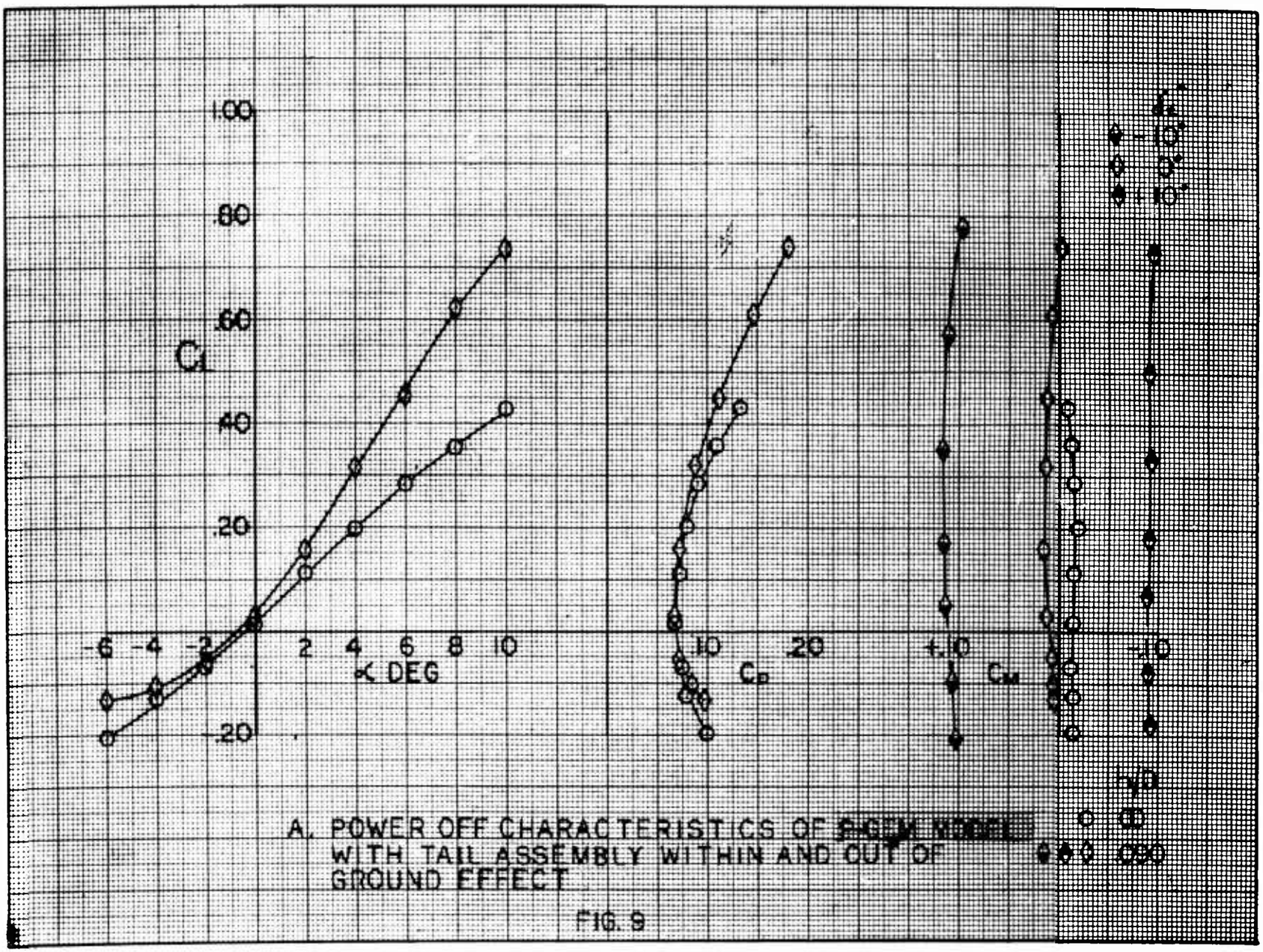

A. POWER OFF CHARACTERISTICS OF [redacted] MODEL WITH TAIL ASSEMBLY WITHIN AND OUT OF GROUND EFFECT

FIG. 9

K·Σ 10 X 10 TO THE CM. KEUFFEL & ESSER CO. 359T-14 MADE IN U.S.A.

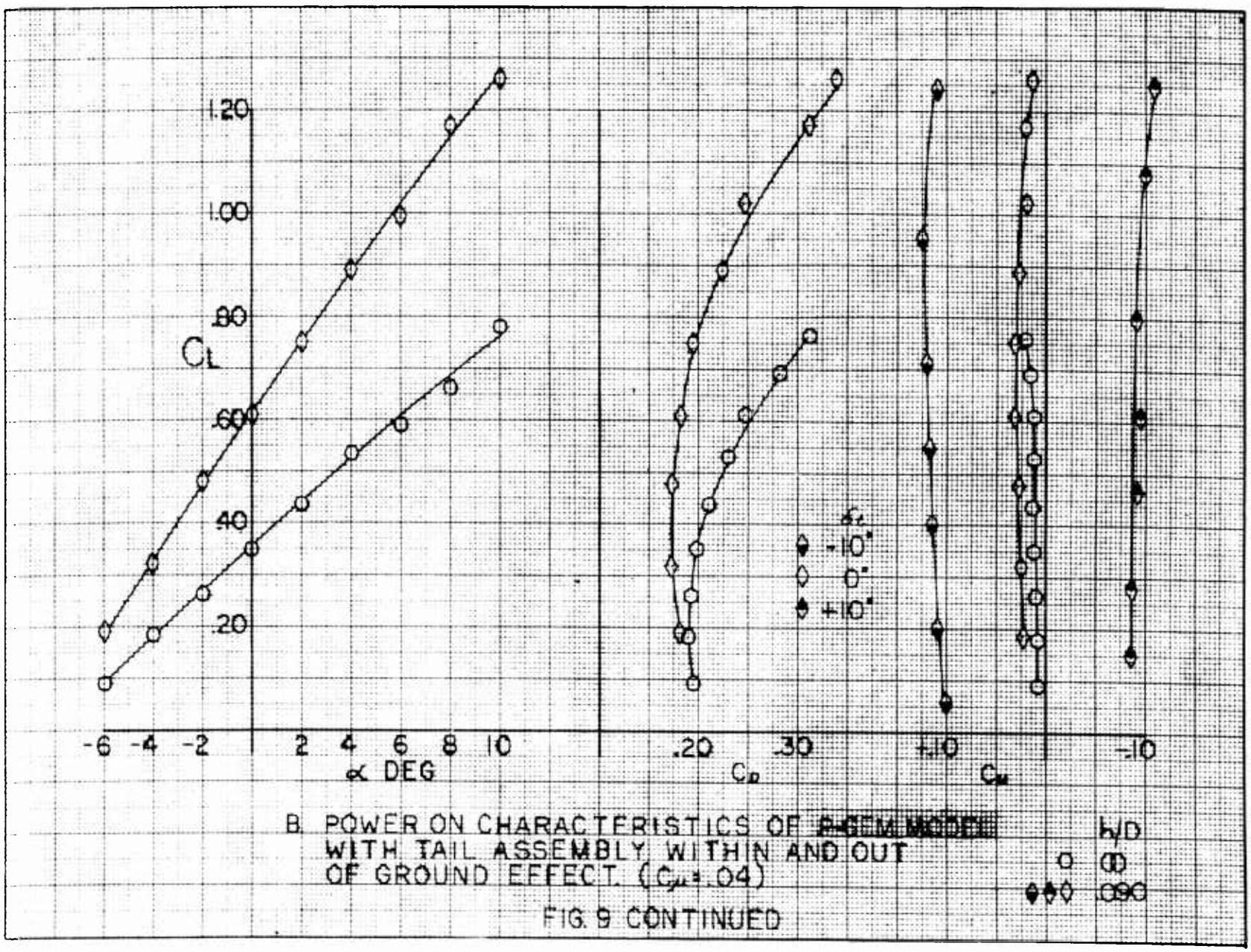

B. POWER ON CHARACTERISTICS OF ~~R-GEM MODEL~~ WITH TAIL ASSEMBLY WITHIN AND OUT OF GROUND EFFECT. (C_μ = .04)

FIG. 9 CONTINUED

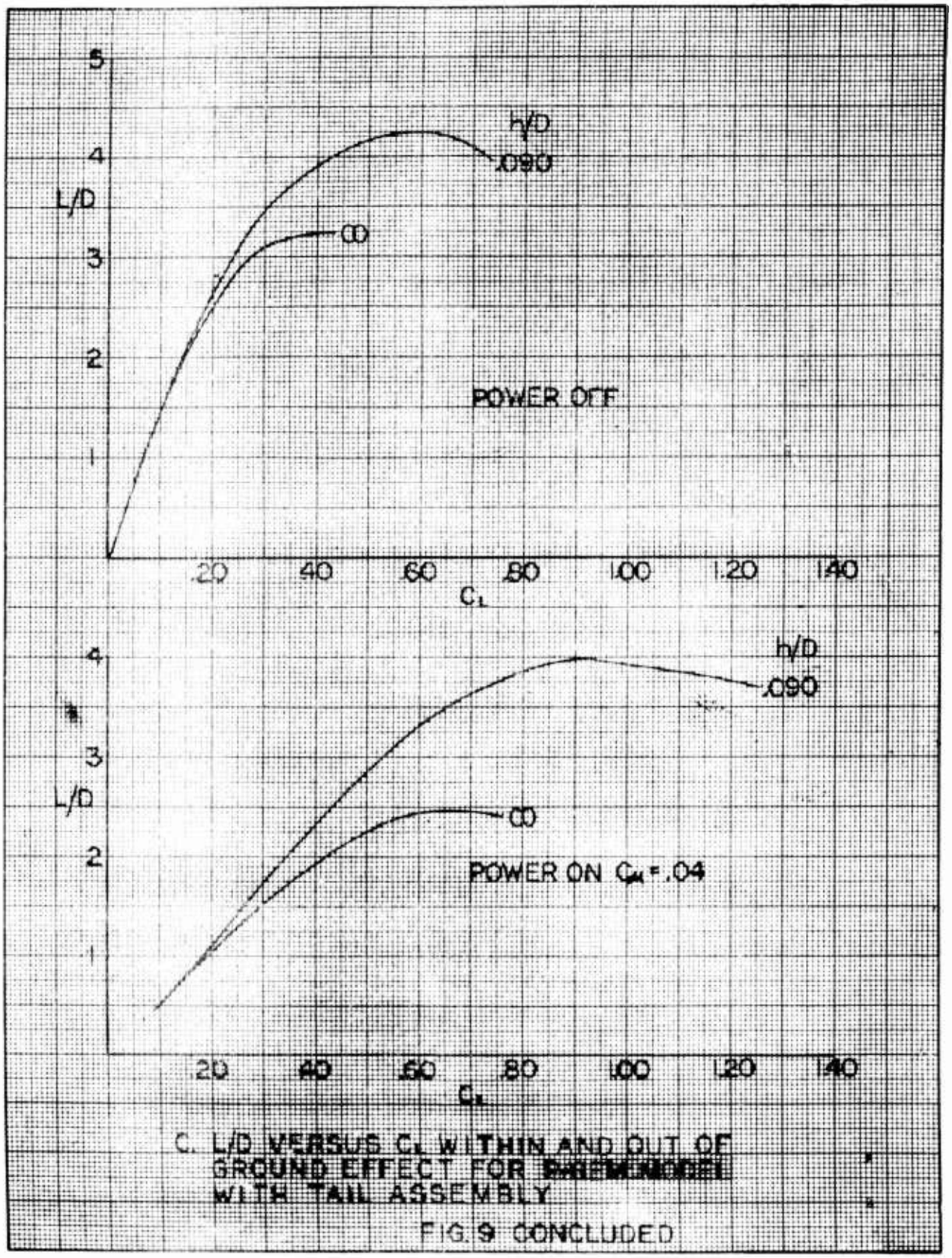

C. L/D VERSUS C_L WITHIN AND OUT OF GROUND EFFECT FOR [redacted] MODEL WITH TAIL ASSEMBLY

FIG. 9 CONCLUDED

K&E 10 X 10 TO THE CM. KEUFFEL & ESSER CO. ALBANENE 359T-14 MADE IN U.S.A.

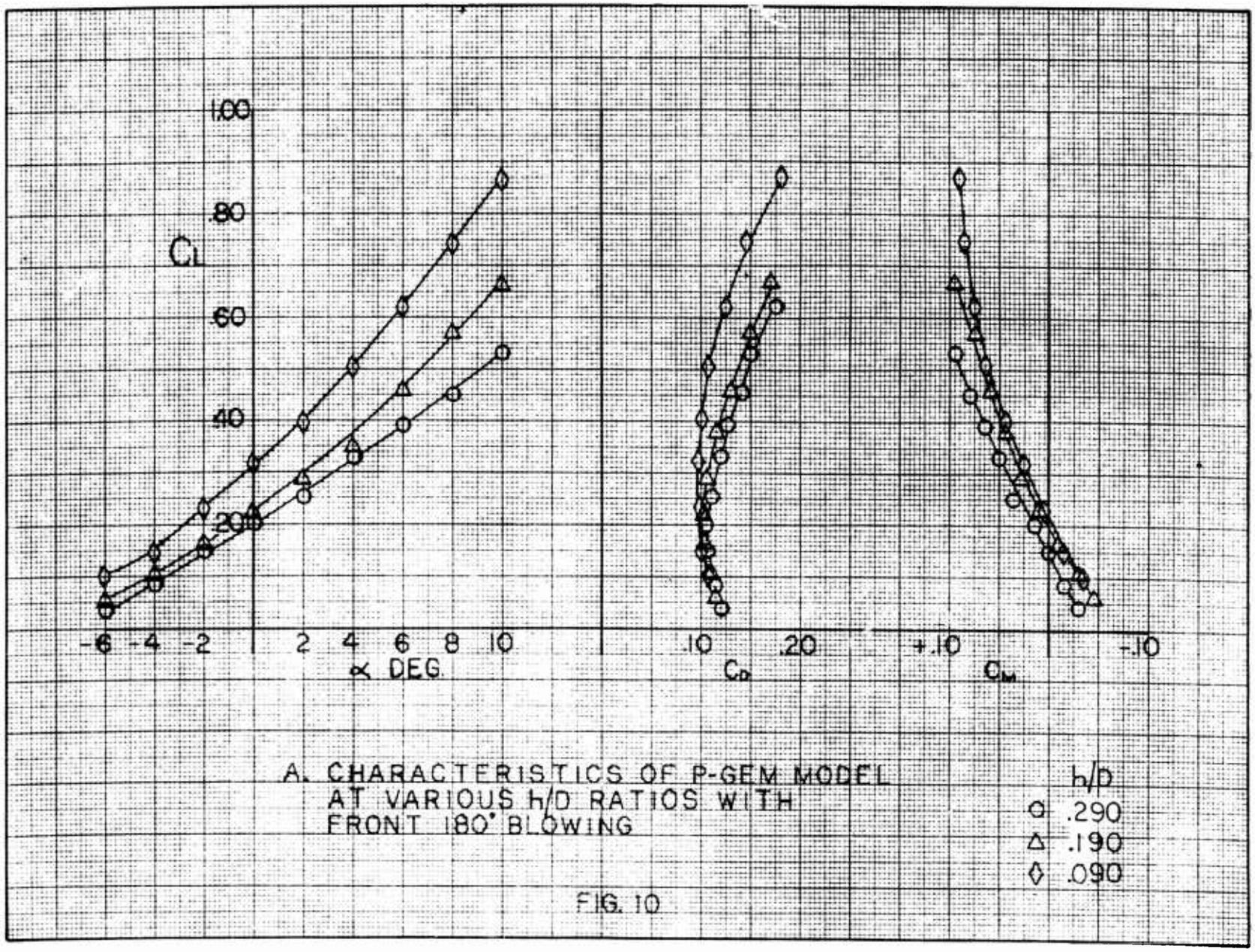

A. CHARACTERISTICS OF P-GEM MODEL AT VARIOUS h/D RATIOS WITH FRONT 180° BLOWING

FIG. 10

K&E 10 X 10 TO THE CM. KEUFFEL & ESSER CO. ALBANENE 359T-14 MADE IN U.S.A.

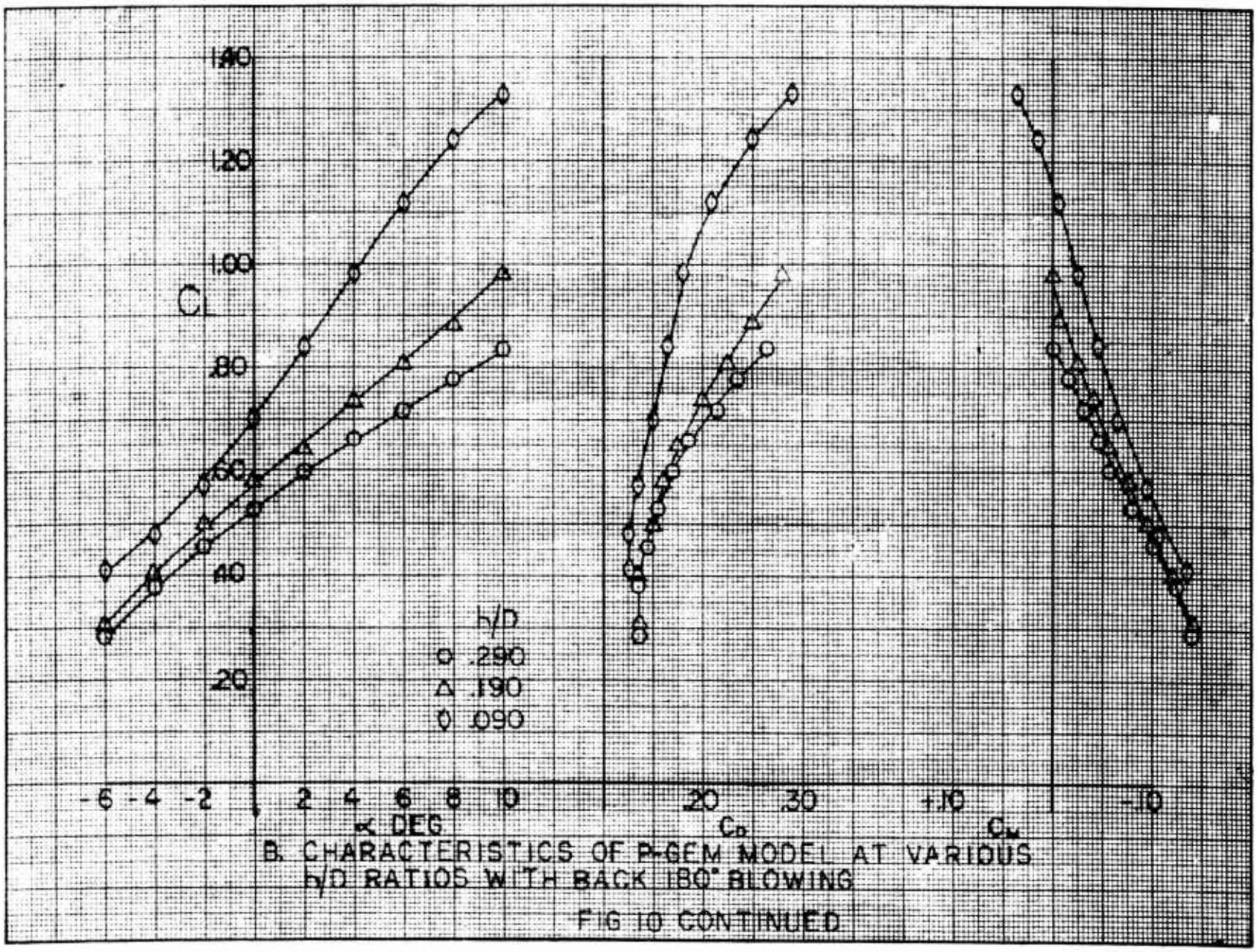

B. CHARACTERISTICS OF P-GEM MODEL AT VARIOUS h/D RATIOS WITH BACK 180° BLOWING

FIG 10 CONTINUED

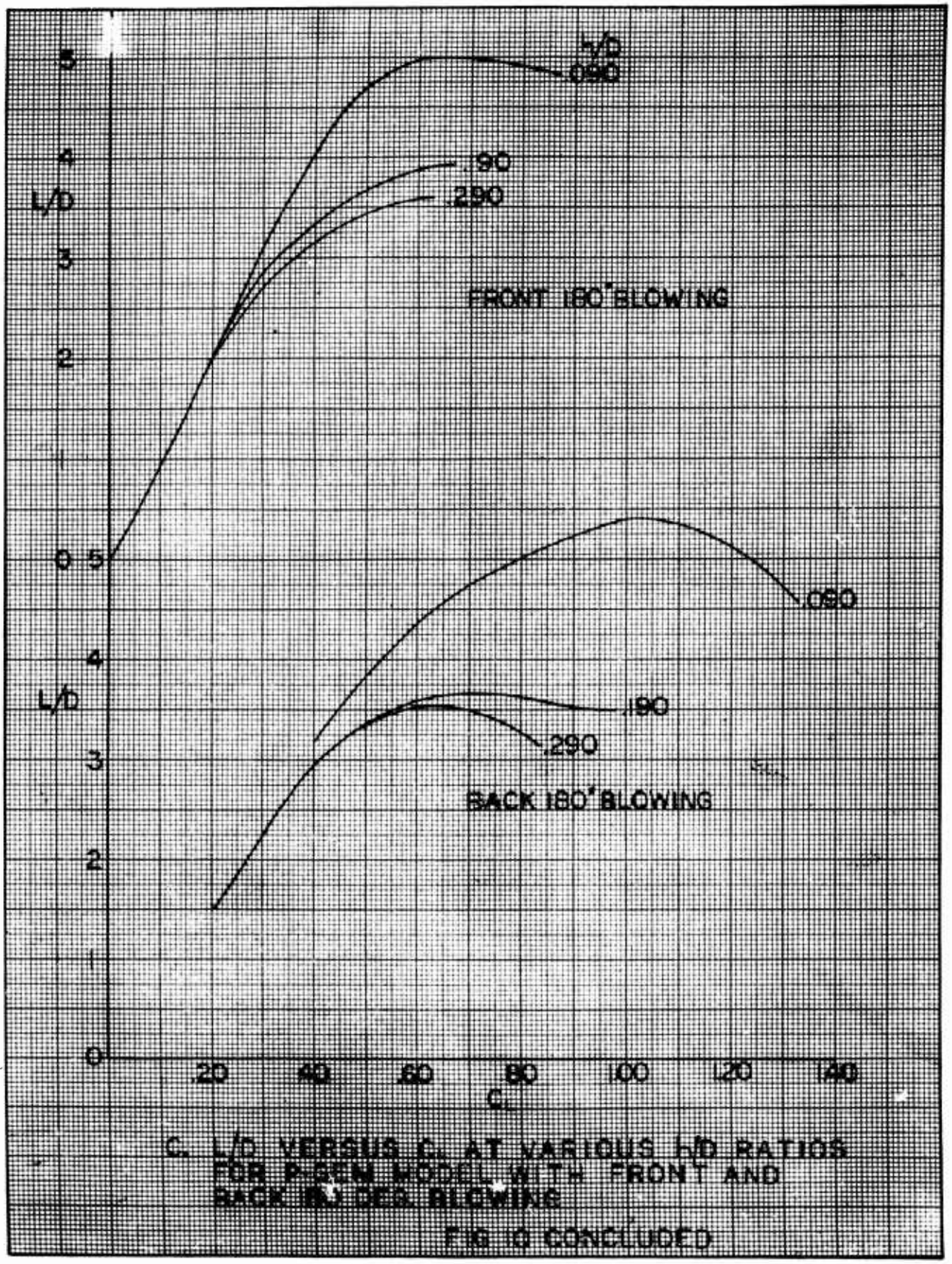

C. L/D VERSUS C_L AT VARIOUS h/D RATIOS FOR P-61A MODEL WITH FRONT AND BACK 180 DEG. BLOWING

FIG 10 CONCLUDED

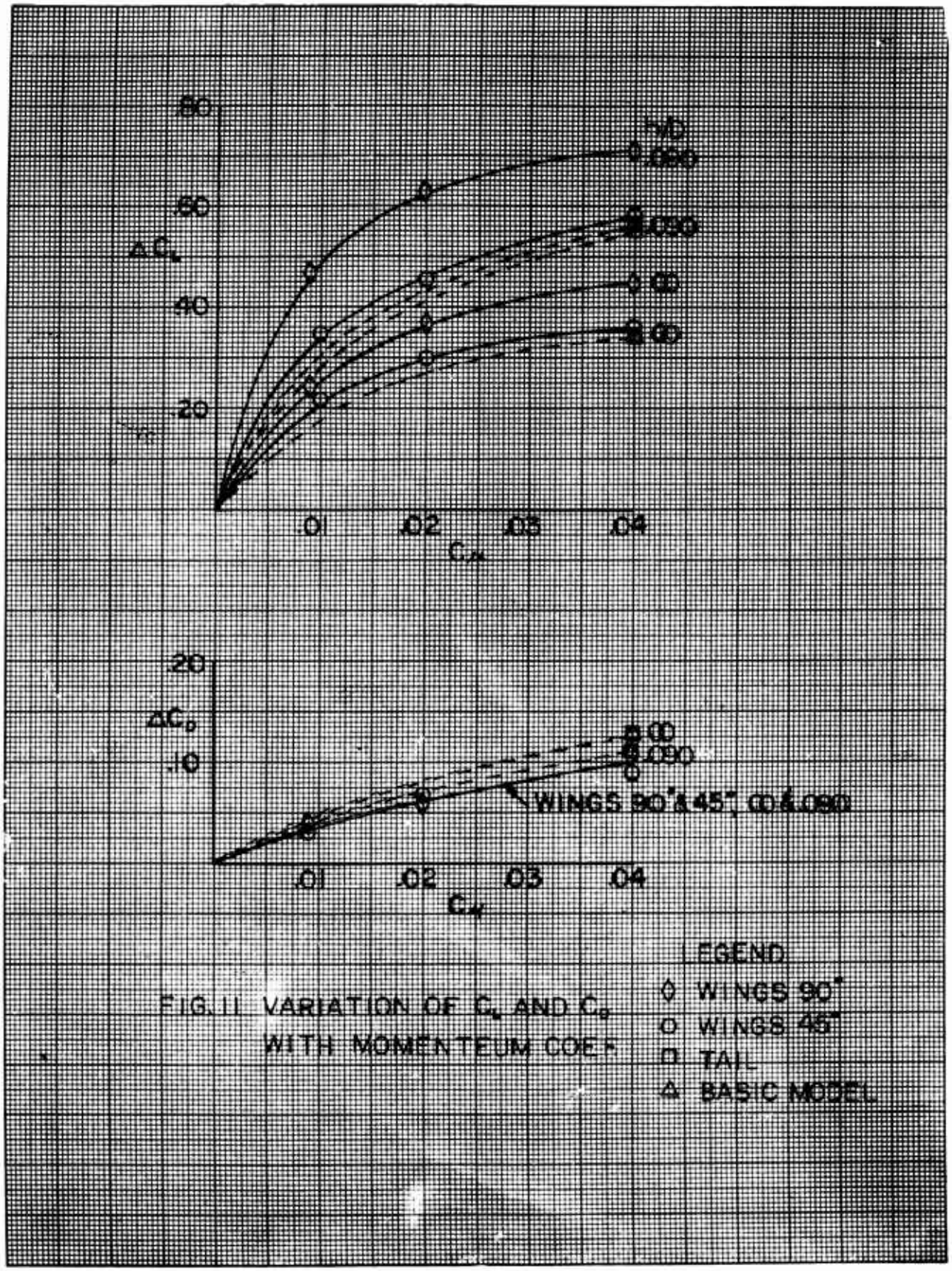

FIG. 11 VARIATION OF C_L AND C_D WITH MOMENTEUM COE.

K·E 10 X 10 TO THE ½ INCH 359-12
KEUFFEL & ESSER CO. MADE IN U.S.A.

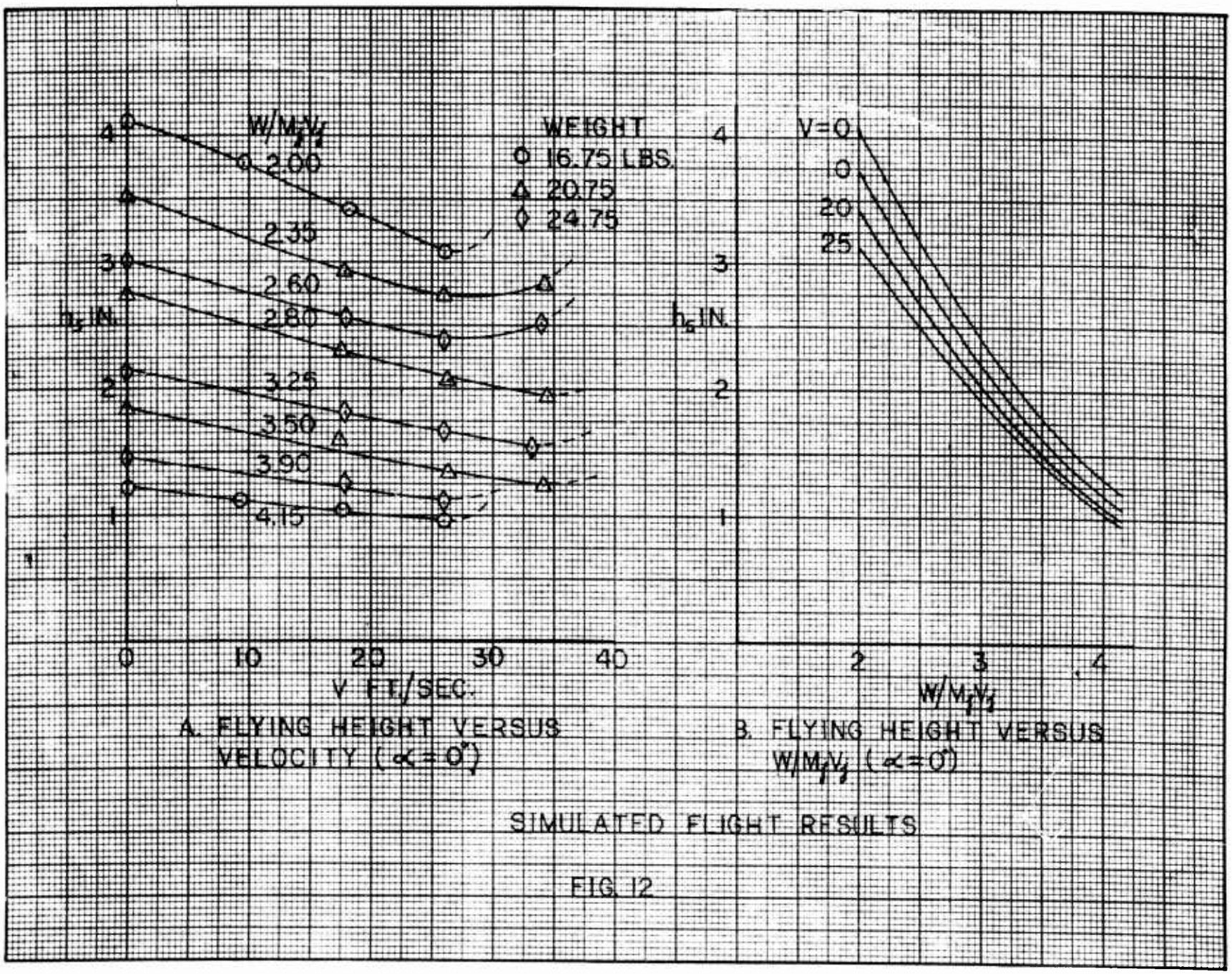

A. FLYING HEIGHT VERSUS VELOCITY ($\alpha = 0°$)

B. FLYING HEIGHT VERSUS $W/M_f V_f$ ($\alpha = 0°$)

SIMULATED FLIGHT RESULTS

FIG. 12

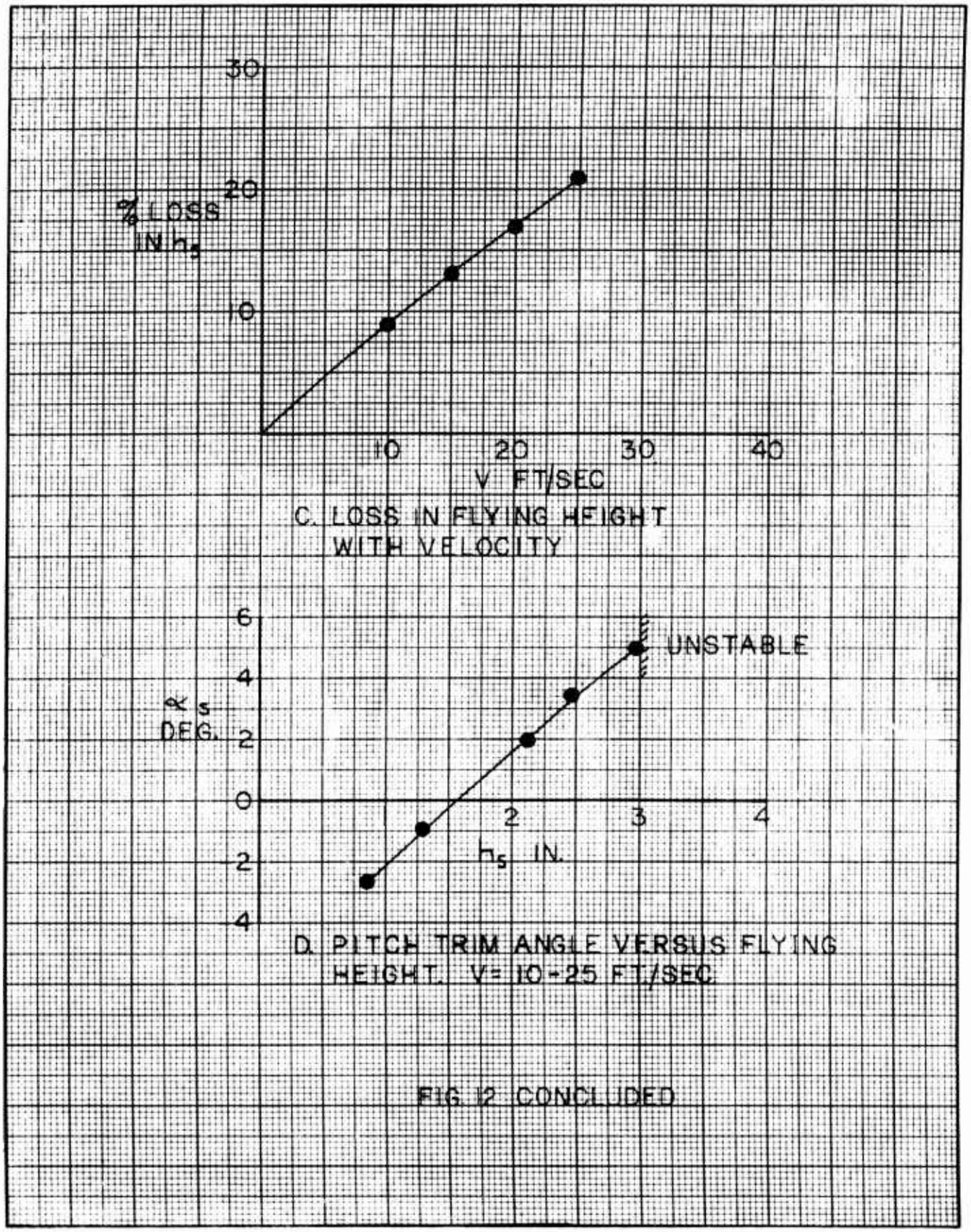

FIG 12 CONCLUDED

359-12
10 X 10 TO THE ½ INCH
KEUFFEL & ESSER CO.

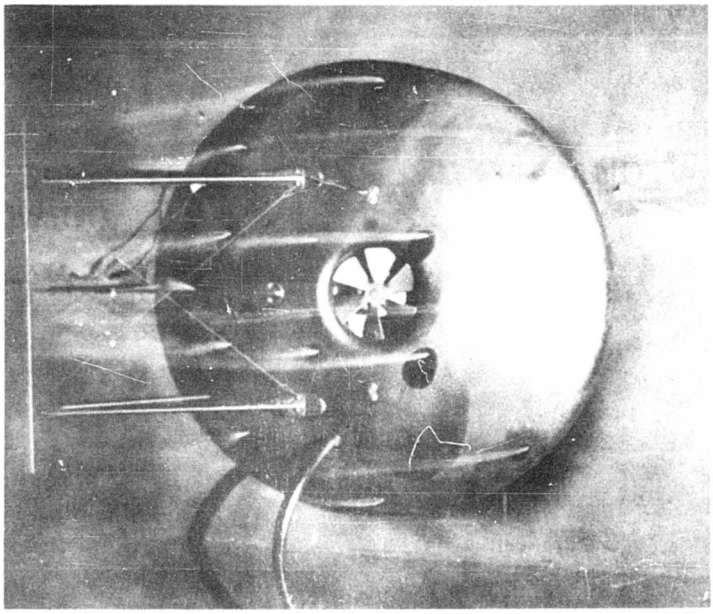

NO BLOWING

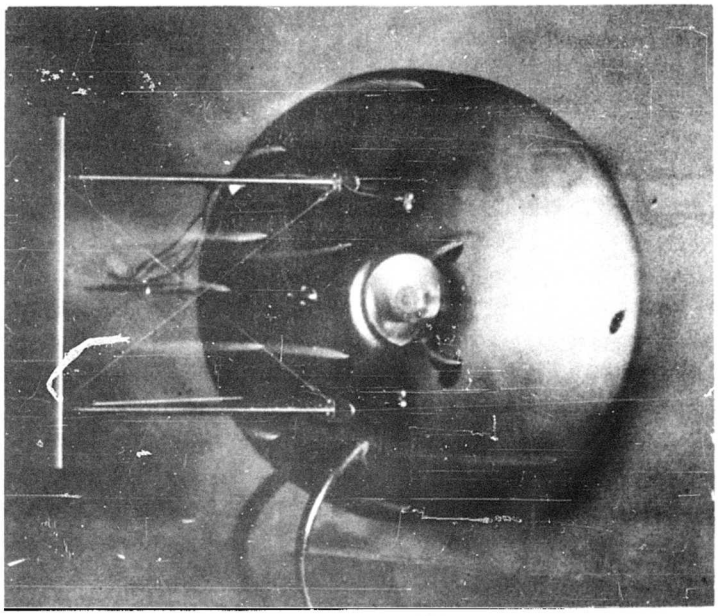

BLOWING

TOPSIDE STREAMLINES WITH AND WITHOUT BLOWING

FIG. 13

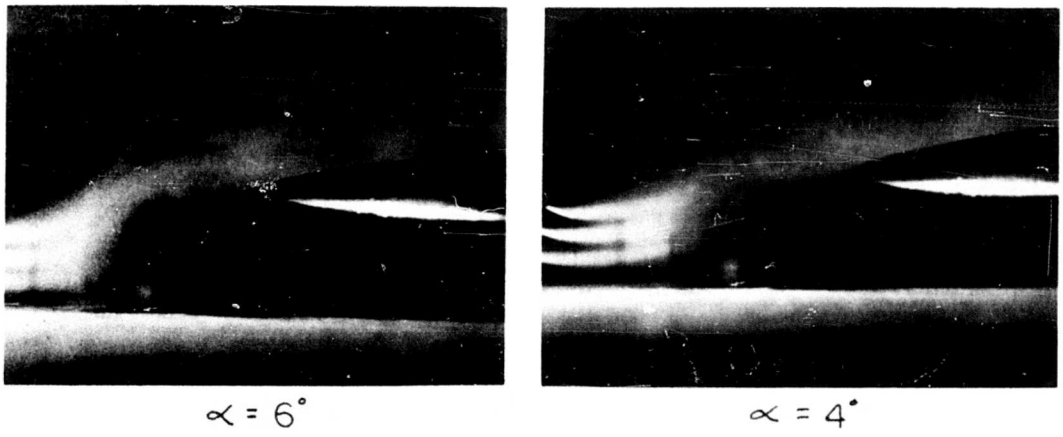

$\alpha = 6°$ $\alpha = 4°$

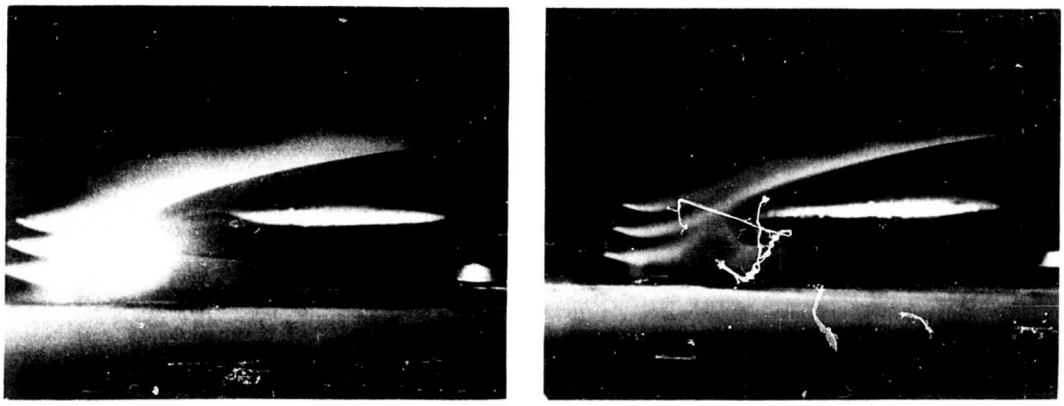

$\alpha = 2°$ $\alpha = 0°$

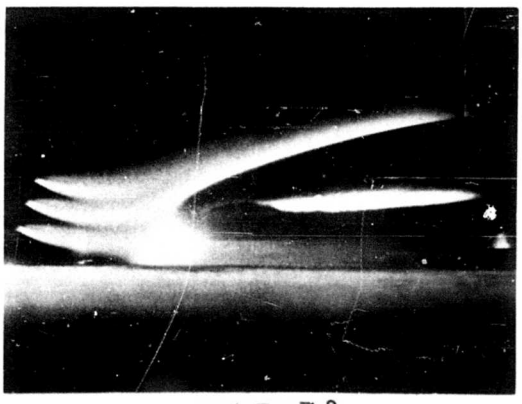

$\alpha = -3°$

A. $g/P_b = .50$, $h/D = .05$

CHANGE IN NOSE VORTEX WITH g/P_b RATIO AND ANGLE OF ATTACK

FIG. 14

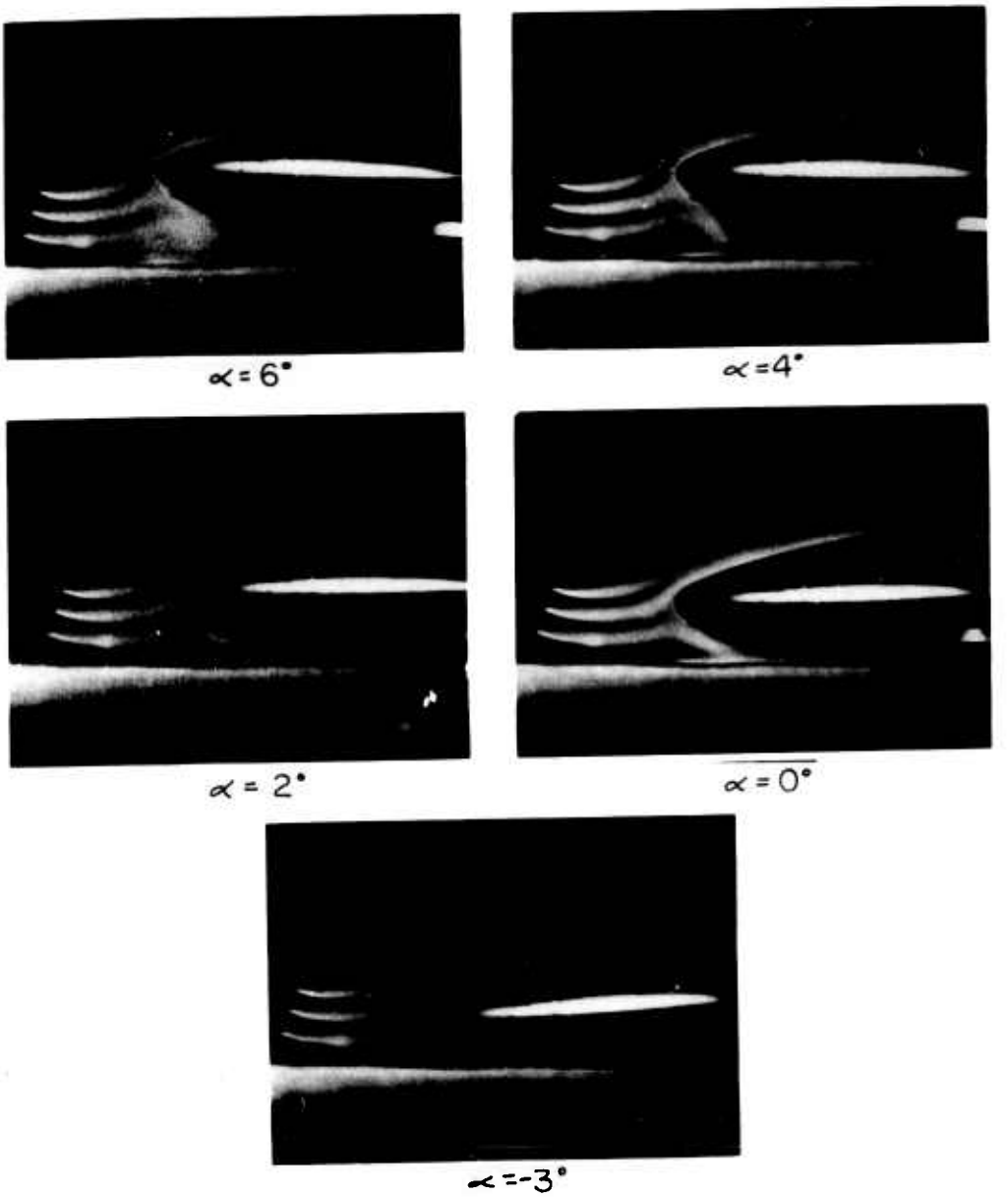

B. $\delta/P_b = .80$, $h/D = .05$

FIG. 14 CONTINUED

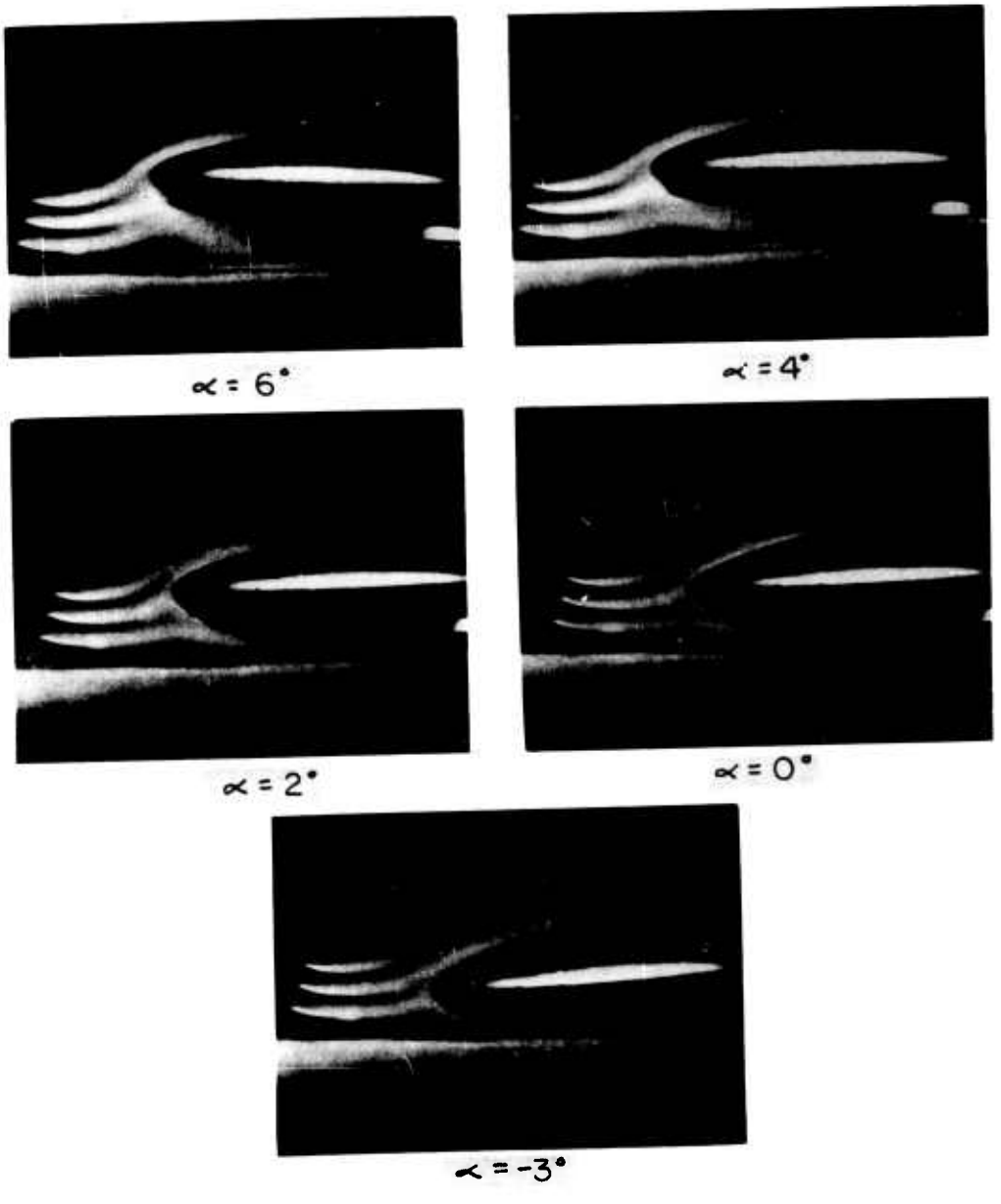

C. $g/P_b = 1.00$, $h/D = .05$

FIG. 14 CONTINUED

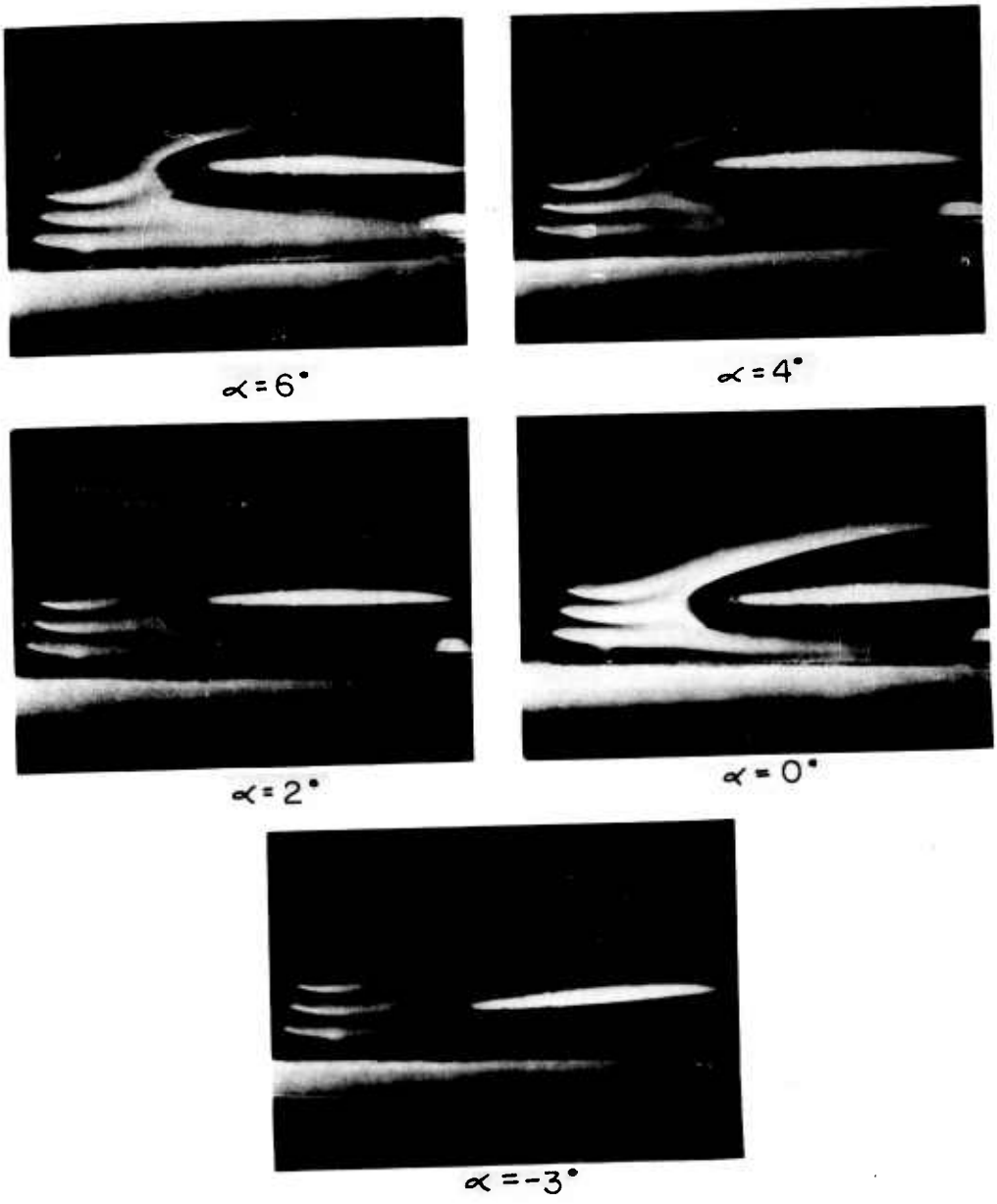

D. $g/R_b = 1.65$, $h/D = .05$

FIG. 14 CONCLUDED

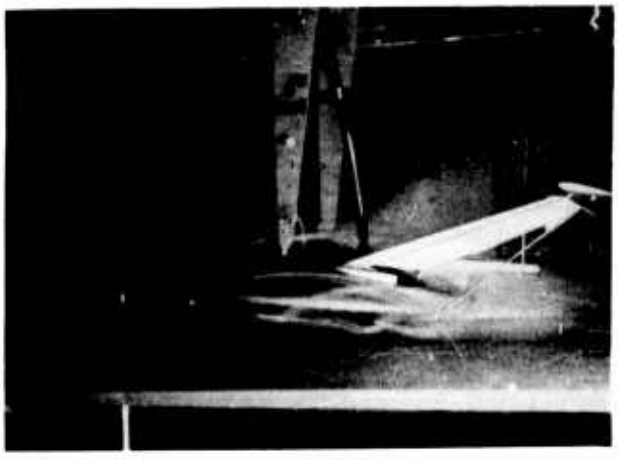

NO BLOWING

BLOWING

SMOKE STUDIES

FIG. 15

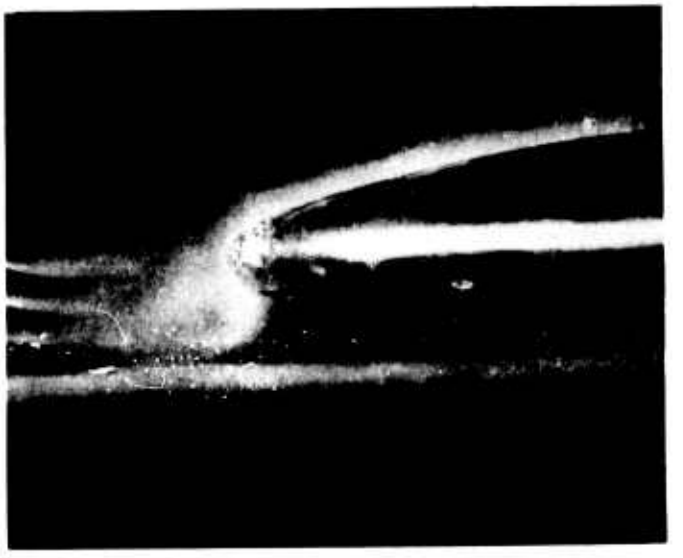

NOSE VORTEX IN DETAIL

FIG. 16

ALART PROGRAM
Technical Report
Distribution List

	ADDRESS	NO. OF COPIES
1.	Chief of Transportaion Department of the Army Washington 25, D. C. ATTN: TCACR	(2)
2.	Commander Wright Air Development Division Wright-Patterson Air Force Base, Ohio ATTN: WCLJA	(2)
3.	Commanding Officer U. S. Army Transportation Research Command Fort Eustis, Virginia ATTN: Research Reference Center ATTN: Aviation Directorate	(4) (3)
4.	U. S. Army Representative HQ AFSC (SCR-LA) Andrews Air Force Base Washington 25, D. C.	(1)
5.	Director Air University Library ATTN: AUL-8680 Maxwell Air Force Base, Alabama	(1)
6.	Commanding Officer David Taylor Model Basin Aerodynamics Laboratory Washington 7, D. C.	(1)
7.	Chief Bureau of Naval Weapons Department of the Navy Washington 25, D. C. ATTN: Airframe Design Division ATTN: Aircraft Division ATTN: Research Division	(1) (1) (1)

	ADDRESS	NO. OF COPIES
8.	Chief of Naval Research Code 461 Washington 25, D. C. ATTN: ALO	(1)
9.	Director of Defense Research and Development Room 3E - 1065, The Pentagon Washington 25, D. C. ATTN: Technical Library	(1)
10.	U. S. Army Standardization Group, U.K. Box 65, U. S. Navy 100 FPO New York, New York	(1)
11.	National Aeronautics and Space Administration 1520 H Street, N. W. Washington 25, D. C. ATTN: Bertram A. Mulcahy Director of Technical Information	(5)
12.	Librarian Langley Research Center National Aeronautics & Space Administration Langley Field, Virginia	(1)
13.	Ames Research Center National Aeronautics and Space Agency Moffett Field, California ATTN: Library	(1)
14.	Armed Services Technical Information Agency Arlington Hall Station Arlington 12, Virginia	(10)
15.	Office of Chief of Research and Development Department of the Army Washington 25, D. C. ATTN: Mobility Division	(1)
16.	Senior Standardization Representative U. S. Army Standardization Group, Canada c/o Director of Weapons and Development Army Headquarters Ottawa, Canada	(1)

	ADDRESS	NO. OF COPIES
17.	Canadian Liaison Officer U. S. Army Transportation School Fort Eustis, Virginia	(3)
18.	British Joint Services Mission (Army Staff) DAQMG (Mov & Tn) 1800 "K" Street, NW Washington 6, D. C. ATTN: Lt. Col R. J. Wade, RE	(3)
19.	Office Chief of Research and Development Army Research Office ATTN: Physical Sciences Division Arlington Hall Station Washington 25, D. C.	(2)
20.	Librarian Institute of the Aeronautical Sciences 2 East 64th Street New York 21, New York	(2)
21.	U. S. Army Research and Development Liaison Group APO 79 New York, New York ATTN: Mr. Robert R. Piper	(1)

AD_____Accession No. ___

Princeton University Aero. Eng. Dept., Princeton, N. J.

MODEL STUDIES OF THE FORWARD FLIGHT CHARACTERISTICS OF THE P-GEM
- M. P. Knowlton and A. F. Wojciechowicz, Jr.

Report No. 581, December, 1961
54 pages

Contract No. DA44-177-TC-524
Project No. 9-38-10-000, TK902
Unclassified Report

UNCLASSIFIED

1. Gr.Ef.Machines Wind Tunnel Tests
2. Gr.Ef.Machines Smoke Tunnel Tests
3. Gr.Ef.Machines Flight Simulation
4. Gr.Ef.Machines Wing, Tail Configurations
5. M.P. Knowlton A. Wojciechowicz
6. Contract No. DA44-177-TC-524

AD_____Accession No. ___

Princeton University Aero. Eng. Dept., Princeton, N. J.

MODEL STUDIES OF THE FORWARD FLIGHT CHARACTERISTICS OF THE P-GEM
- M. P. Knowlton and A. F. Wojciechowicz, Jr.

Report No. 581, December, 1961
54 pages

Contract No. DA44-177-TC-524
Project No. 9-38-10-000, TK902
Unclassified Report

UNCLASSIFIED

1. Gr.Ef.Machines Wind Tunnel Tests
2. Gr.Ef.Machines Smoke Tunnel Tests
3. Gr.Ef.Machines Flight Simulation
4. Gr.Ef.Machines Wing, Tail Configurations
5. M.P. Knowlton A. Wojciechowicz
6. Contract No. DA44-177-TC-524

AD_____Accession No. ___

Princeton University Aero. Eng. Dept., Princeton, N. J.

MODEL STUDIES OF THE FORWARD FLIGHT CHARACTERISTICS OF THE P-GEM
- M. P. Knowlton and A. F. Wojciechowicz, Jr.

Report No. 581, December, 1961
54 pages

Contract No. DA44-177-TC-524
Project No. 9-38-10-000, TK902
Unclassified Report

UNCLASSIFIED

1. Gr.Ef.Machines Wind Tunnel Tests
2. Gr.Ef.Machines Smoke Tunnel Tests
3. Gr.Ef.Machines Flight Simulation
4. Gr.Ef.Machines Wing, Tail Configurations
5. M.P. Knowlton A. Wojciechowicz
6. Contract No. DA44-177-TC-524

AD_____Accession No. ___

Princeton University Aero. Eng. Dept., Princeton, N. J.

MODEL STUDIES OF THE FORWARD FLIGHT CHARACTERISTICS OF THE P-GEM
- M. P. Knowlton and A. F. Wojciechowicz, Jr.

Report No. 581, December, 1961
54 pages

Contract No. DA44-177-TC-524
Project No. 9-38-10-000, TK902
Unclassified Report

UNCLASSIFIED

1. Gr.Ef.Machines Wind Tunnel Tests
2. Gr.Ef.Machines Smoke Tunnel Tests
3. Gr.Ef.Machines Flight Simulation
4. Gr.Ef.Machines Wing, Tail Configurations
5. M.P. Knowlton A. Wojciechowicz
6. Contract No. DA44-177-TC-524

A wind tunnel investigation has been conducted to determine the forward flight characteristics of a 1/12 scale model of the P-GEM. Separate studies were also made of the model with non-blowing wings attached at several locations around its perimeter and also with the addition of a tail.

Flight simulation studies were made using a 1/5 scale model of the P-GEM to determine the nature of height decay with weight to momentum thrust ratio and velocity. Additional studies were made to investigate the change in pitch trim and stability with flying height.

Smoke studies of the 1/12 scale model were made to investigate the vortex formation and streamline flow at various dynamic to base pressure ratios.

A wind tunnel investigation has been conducted to determine the forward flight characteristics of a 1/12 scale model of the P-GEM. Separate studies were also made of the model with non-blowing wings attached at several locations around its perimeter and also with the addition of a tail.

Flight simulation studies were made using a 1/5 scale model of the P-GEM to determine the nature of height decay with weight to momentum thrust ratio and velocity. Additional studies were made to investigate the change in pitch trim and stability with flying height.

Smoke studies of the 1/12 scale model were made to investigate the vortex formation and streamline flow at various dynamic to base pressure ratios.

A wind tunnel investigation has been conducted to determine the forward flight characteristics of a 1/12 scale model of the P-GEM. Separate studies were also made of the model with non-blowing wings attached at several locations around its perimeter and also with the addition of a tail.

Flight simulation studies were made using a 1/5 scale model of the P-GEM to determine the nature of height decay with weight to momentum thrust ratio and velocity. Additional studies were made to investigate the change in pitch trim and stability with flying height.

Smoke studies of the 1/12 scale model were made to investigate the vortex formation and streamline flow at various dynamic to base pressure ratios.

A wind tunnel investigation has been conducted to determine the forward flight characteristics of a 1/12 scale model of the P-GEM. Separate studies were also made of the model with non-blowing wings attached at several locations around its perimeter and also with the addition of a tail.

Flight simulation studies were made using a 1/5 scale model of the P-GEM to determine the nature of height decay with weight to momentum thrust ratio and velocity. Additional studies were made to investigate the change in pitch trim and stability with flying height.

Smoke studies of the 1/12 scale model were made to investigate the vortex formation and streamline flow at various dynamic to base pressure ratios.

UNCLASSIFIED

UNCLASSIFIED